Review

NIR/AIE Fluorescent Probes for Its Specific Detection Towards H_2O_2: Design Strategies, Applications and Outlook

Gunasekaran Prabakaran *, Suguna Sivasubramanian , Krishnasamy Velmurugan *

Posted Date: 7 July 2025

doi: 10.20944/preprints202507.0403.v1

Keywords: NIR probes; H_2O_2; biological applications

 doi:10.20944/preprints202507.0403.v1

Review

NIR/AIE Fluorescent Probes For its Specific Detection Towards H_2O_2: Design Strategies, Applications and Outlook

Gunasekaran Prabakaran [1,2], Suguna Sivasubramanian [3] and Krishnasamy Velmurugan [4,*]

[1] Institute for Advanced Study, Shenzhen University, Shenzhen 518060, China
[2] School of Physics and Optoelectronic Engineering, Shenzhen University, Shenzhen 518060, China
[3] Department of Science & Humanities, Karpagam college of Engineering, Myleripalayam, -641032
[4] College of Materials Science and Technology, Nanjing University of Aeronautics and Astronautics, Nanjing 211106, China
* Correspondence: velu117@nuaa.edu.cn

Abstract

The presence of superoxide dismutase and various oxidases in cells indicates that hydrogen peroxide (H_2O_2), which acts as a signaling molecule closely linked to numerous biological activities. The presence of hydroxyl radicals in their moiety is also responsible for biological harm, contributing to the development of significant illnesses such as fatty liver disease, cancer, and inflammation. To mitigate the risk of early-stage research complications, it is essential to develop advanced NIR fluorescent probes, which are capable of detecting diseases associated with H_2O_2 Therefore, in this review mainly focuses on the basic design and recent development of NIR probes (400–700 nm), NIR-I probes (700–900 nm), and NIR-II probes (900–1700 nm) for the detection of H_2O_2 in biological system. In addition, sensing methodologies and reaction mechanisms were explained with the help of both colorimetric and fluorimetric techniques as reported by researchers. Furthermore, we examined the potential mechanisms and application of NIR fluorescent probes that are capable of recognizing H_2O_2 in biological environments. potential challenges, opportunities and future trends in the field of NIR probe design and sensing of H_2O_2 will also be discussed.

Keywords: NIR probes; H_2O_2; biological applications

1. Introduction

Hydrogen peroxide (H_2O_2) in the reactive oxygen species (ROS) system contributes to the cell growth and proliferation of cells [1–4]. Compared with other ROS-based derivatives, H_2O_2 has an advantage over intracellular hydrogen peroxide, which is primarily produced by the endoplasmic reticulum, mitochondria, and a variety of oxidases. Abnormal production of H_2O_2 caused Alzheimer's disease (AD), diabetes, cancer, cardiovascular disorders, and inflammatory diseases [5–7]. In addition to that it plays a significant role in a broad variety of pathological and physiological consequences occurred in the living organisms. Therefore, the development of near infrared (NIR) fluorescence probes for the detection of H_2O_2 can potentially contribute to human health via the use of biological applications [8–11].

NIR probes have become more important for the detection of analytes because of its unparalleled, an exceptional sensitivity, real-time imaging and visualization under the naked eye or UV light. [18–21]. As a result, there has been a rise in the development of NIR-based fluorescent probes for the precise detection of H_2O_2 in live cells and animals via the use of imaging methods. [22–25].

 doi:10.20944/preprints202507.0403.v1

Development of NIR fluorescent probes usually composed of a binding site, a connecting arm and a strong fluorophore attached to it. Here, fluorophore acts as a singling unit in the NIR region. Recently, various fluorophores have been used for the design and development of NIR emission based fluorescent probes namely rhodamine, cyanine, tetraphenylethylene (TPE), triphenylamine (TPA), quinoline, boron-dipyrromethene and other aldehyde based derivatives [26–33]. The probes interaction between recognition unit and analyte depends on two different ways: i) activity based probes ii) binding based probes. In this case, the interaction depends upon the recognition unit and analytes combined with the developed NIR fluorescent probes is a common way [34,35]. In this strategy, signal to noise fluorescence imaging requires turn-on fluorescent probes that washed away repeatedly in cell imaging applications. Another strategy is key-lock interaction, which has high specificity towards target analyte in the physiological environment and can avoid impaired complexation. At the same time, if the developed fluorescent probe has a special conformation in its structure, which could avoid impairing complexation. Before complexation with target analyte, these type of probes are non-emissive in nature [36,37]. After complexation with analyte, recognition unit of the probe could enhance the fluorescence signal due to its conformational changes and structural rigidity. This review focuses on a basic design and development of NIR probes as reported by various research groups. Designing of NIR probes can be classified into three distinct methods. In type I, a fluorescent probe acts as a non-emissive in nature, which is restored by the recognition of a specific analyte. This process could be explained by the supporting of various mechanisms, such as PET, ICT and FRET processes [38–42].In Type-II NIR probes possess reaction sites, which are precisely triggered in the presence of target analytes followed by increase their fluorescence [43–46]. This activation takes place either by the restriction of intramolecular motion (RIM) or through the cleavage of the identifying sites accomplished through the ICT process. In type III, the probe went through a structural rearrangement as a result of the cleavage of the identifying unit, which resulted in a significant NIR emission[47–49].

2. Different Types of Fluorophores Used to Detect H_2O_2

2.1. Tetraphenylamine (TPA) & Tetraphenylethylene (TPE) Based Probes

Most of the TPA derivatives transmit charges and provide remarkable efficiency. Therefore, these derivatives have been used as crucial components in the area of optoelectronics. Due to the fact that high charge mobility is necessary for optimum device performance, organic field-effect transistors (OFETs) and organic light-emitting diodes (OLEDs) make substantial use of them. TPE derivatives are distinguished by their emission phenomena, which are impacted by aggregation. At larger concentrations, many fluorescent materials undergo quenching, while TPE displayed strong emission by aggregation. Because of this feature, they are widely used in sensors and bioimaging applications.

Li Fan et al. synthesized a near-infrared (NIR) fluorescent probe **1** for the specific detection of hydrogen peroxide (H_2O_2), which exhibited orange fluorescent emission [50]. Prior to the treatment, probe 1 exhibited weak fluorescence attributed to unrestricted rotation within the mito-targeting structure. Upon the addition of H_2O_2 to probe 1, the phenylboronic acid group underwent cleavage, resulting in the restricted rotation of ……. This alteration provided a strong fluorescence at 588 nm. As the concentration of H_2O_2 increased, a gradual rise in fluorescence emission was observed, followed by a color transition from colorless to an orange under UV light at 365 nm. Dong Wang et al. developed a similar NIR probe **2** for the detection of H_2O_2 using colorimetric and fluorimetric methods [51]. In colorimetric analysis, probe 2 exhibited a strong absorption band at 400 nm. Upon the addition of H_2O_2, band at 400 nm was disappeared resulting in the emergence of a new peak at 490 nm. Conversely, addition of H_2O_2 to **2**, fluorescence enhancement was observed with 37.5-fold increase. a color change was observed with the naked eye and under UV light, confirming the complexation of H_2O_2 with probe 2.

 doi:10.20944/preprints202507.0403.v1

Zhiqiang Mao and his team developed a Cys-triggered fluorescent probe **3** for use in complexation in the presence of H_2O_2 during apoptosis [52]. NIR fluorescent probe (add number) was selectively binding to Cys as evidenced by both colorimetric and fluorimetric titration techniques. As the concentration of Cys increased, probe 3 exhibited a strong fluorescence and saturated within 45 min. The complexation underwent additional treatment in the presence of H_2O_2, a substance frequently utilized to induce apoptosis via oxidative stress. PC12 and HepG2 cell lines were subjected to treatment with Cys in the context of an H_2O_2-induced apoptotic model. The results demonstrated that the H_2O_2-treated cells exhibited a shrivelled appearance in comparison to the control, attributed to the oxidation process of H_2O_2. The apoptotic rate increased in both PC12 and HepG2 cells during H_2O_2 incubation when treated with probe 3 in the presence of Cys. As shown in Figure 1, probes 1 and 2 did not exhibit fluorescence in HeLa cells. However, addition of H_2O_2 with varying concentration resulted in a gradual increase of the orange and yellow fluorescence. Additionally, live tissue culture was employed to identify H_2O_2 using probe 1.Tumor-containing region exhibited pronounced orange fluorescence in the H_2O_2 channel and NIR emission in the viscosity channel.

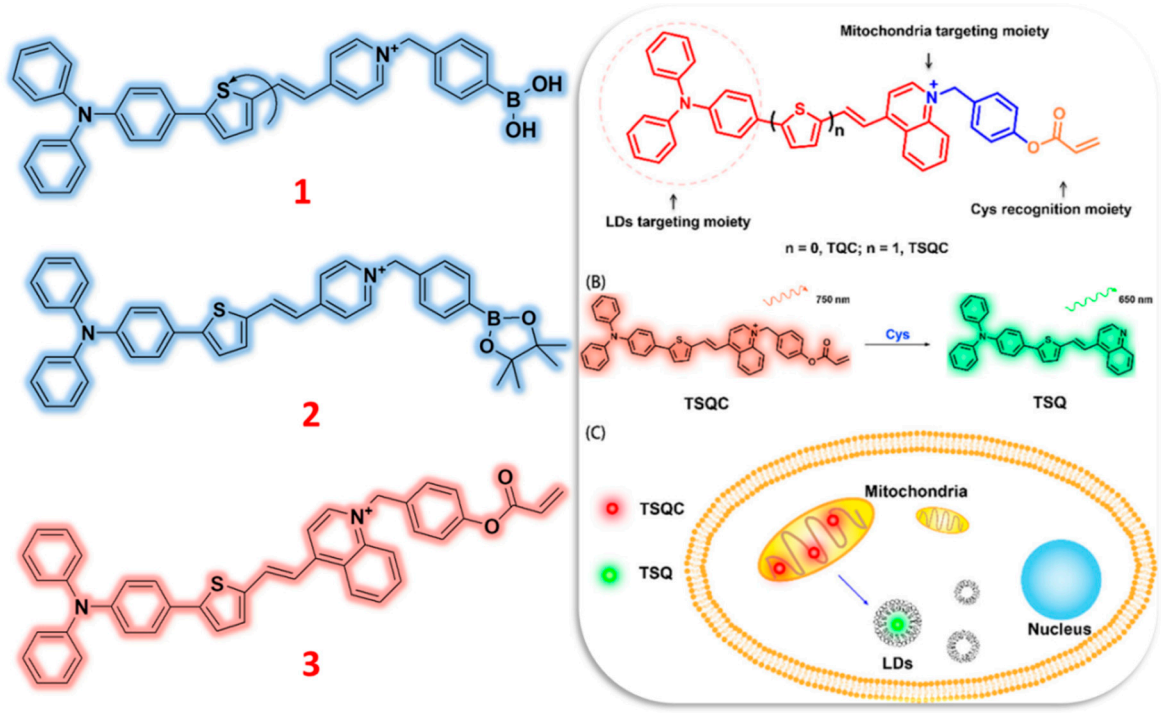

Figure 1. Structure of Tetraphenylamine (TPA) based fluorescent probes (**1-3**) for the detection of H_2O_2 ions and graphical illustration of probe **3** for its applications in detection H_2O_2 in mitochondria and liquid droplets. Reproduced with permission from Refs. [52], Copyright, American Chemical Society.

Lei Yang and their research group developed a NIR dual-channel fluorescent probe **4** for the selective detection of hydrogen peroxide, with the complexation further applied for visualization purposes [53]. Probe 4 exhibited non-fluorescence due to the photoinduced electron transfer (PET) process. Upon treatment with H_2O_2 and other ions, H_2O_2 exhibited a significant fluorescence enhancement at 550 nm. This was due to the cleavage of p-phenylboronic acid from probe 4 followed by inhibition of the PET process. A novel AIE-gen based fluorescent probe **5** was synthesized and characterized for its high responsiveness to H_2O_2 [54]. Probes were subjected to various analytes, probe 5 exhibited a significant blue-shifted fluorescence (740 nm to 525 nm) with increase of 200-fold in the presence of H2O2. Meanwhile, color transition was observed from pale green to pink. This change confirmed the binding interaction between H_2O_2 and probe 5. Additionally, the color change technique of probe 5 was applied in the RGB color assist application. Two distinct AIE-gen TPE-based fluorescent probes **6** and **7** were developed for the specific detection of H_2O_2. These probes are utilized

 doi:10.20944/preprints202507.0403.v1

to assess the health status of plants, identify its presence in foodstuffs, and imaging applications as reported by Shuai Zhang et al. and Lijun Tang et al [55,56]. Initially, Shuai Zhang and their research team synthesized various derivatives of TPE. All TPE derivatives exhibited strong fluorescence; however, addition of H_2O_2, a reduction in fluorescence was observed. Among the developed TPE-derived probes, only probe 6 exhibited a significant quenching effect with color change from blue to light blue. The probe 6 was subjected to testing with various analytes and organic compounds. Results indicated that probe 6 exhibited strong emission in the presence of other analytes, demonstrating its capability to selectively detect H_2O_2. Lijun Tang et al. developed a robust AIE-gen fluorescent probe for the detection of H_2O_2 in food products and bioimaging applications. probe 7 exhibited weak fluorescence. However, upon treatment with H_2O_2, there was a significant enhancement in fluorescence intensity. With an increase in the concentration of H_2O_2, there was a gradual increase in the fluorescence intensity of probe 7, accompanied by color changes from blue to pink under UV-365nm and from pale yellow to colorless in naked eye. These results attributed to the introduction of H_2O_2 to probe 7, resulting in the regeneration and restoration of the original characteristics of probe 7, as confirmed through NMR and ESI-MS. TPA and TPE based fluorescent probes were applied to various cell lines and live tissue cultures. Subsequently, probes 4 and 5 were applied to HepG2 cell lines, living mice, and zebrafish for the detection of H_2O_2 in the presence of various staining components. Probe 4 exhibited significant fluorescence emission in both the green and red channels. However, this emission was substantially quenched in the presence of H_2O_2. Notably, after pre-treatment with LPS, the robust fluorescence of probe 4 was reinstated, indicating its potential application in the treatment of inflammation in mice (Figure 2). Probe 5 underwent identical treatment protocols when applied to HepG2 cell lines and zebrafish models. Probe 5 exhibited strong emission in both the red and green channels for the HepG2 cell line and zebrafish. In contrast, addition of H2O2 showed a gradual decrease of its emission. Probes 6 and 7 were applied to plant tissue and MCF-7 cell lines. Probe 6 was applied to Orin apple calli cells, which initially exhibited a weak fluorescence in the green channel. Following the addition of NaCl stress, the green signal became apparent after the removal of the stressor. This observation confirmed that probe 6 could be applied for detecting H_2O_2 in both cells and plants. Conversely, probe 7 with MCF-7 cell lines exhibited strong emission in the red channel. Upon the introduction of HSO_3^- ions, emission was ceased entirely due to quenching effect. However, upon the subsequent addition of H_2O_2 to the same medium, emission was restored to its original intensity in the red channel. This result demonstrated that probe 7 could be effectively utilized for the detection of both HSO_3^- and H_2O_2 in cells.

 doi:10.20944/preprints202507.0403.v1

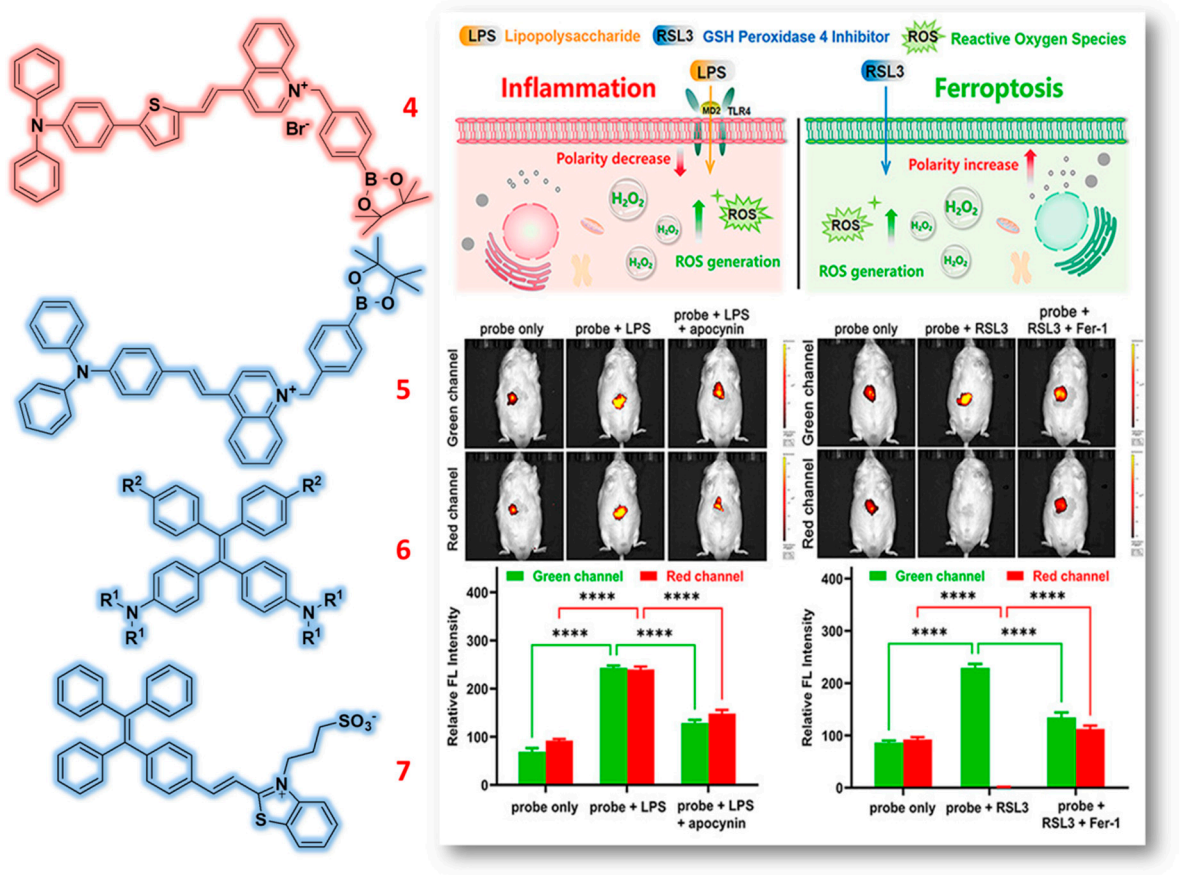

Figure 2. Structure of TPA and TPE-based fluorescent probes (**4-7**) for the selective sensing of H_2O_2 ions. Diagram of the construction of probe **4** and its applications against inflammation and ferroptosis mice. Reproduced with permission from Refs. [53], Copyright, American Chemical Society.

2.2. Quinoline & Quinolinium Based Probes

Quinoline, a heterocyclic aromatic compound, is an excellent fluorophore due to its unique structural and electronic properties. This has made it a popular choice for developing fluorescent probes that selectively detect and bind to specific metal ions. These quinoline-based probes have been successfully employed in various applications, including detecting metal ions in food samples and biological systems. The derivatives of quinoline, with their exceptional quantum yield and high fluorescent intensity, have garnered significant interest, offering promising avenues for further research and practical applications in analytical chemistry and bioimaging. Quinolinium dyes and salts are a class of fluorescent probes that have demonstrated exceptional versatility in various medical applications. These compounds have shown significant efficacy in detecting and treating different diseases. Additionally, they have proven valuable in identifying harmful ions in food samples and provide numerous advantages for real-time monitoring applications. Designed for on-site monitoring and biological uses, Haixia Zhang and colleagues developed a new near-infrared fluorescence probe for the dual detection of hydrogen peroxide in oxidative stress and hydrogen sulfide ions [57]. Using both colorimetric and fluorimetric titration approaches, the produced probe **8** was tested with many analytes. Probe 8 showed a significant absorption band and strong fluorescence emission in their natural form as an NIR probe. Nevertheless, both techniques showed a notable new absorption peak in absorbance and a quenching impact in fluorescence emission following H_2O_2 addition. Probe 8 with H_2O_2 showed a little rise in fluorescence intensity and a drop in absorbance during the sequential investigations on complexation in the presence of H_2S. Under both techniques, H_2S produced a red shift followed by a blue to yellow color change. Lingliang Long et al. created a probe **9** for cell imaging methods and selective H_2O_2 detection in food samples [58]. In

 doi:10.20944/preprints202507.0403.v1

its natural form, the produced probe 9 showed weak fluorescence emission and significant absorption bands. On the other hand, a drop in absorbance and a rise in fluorescence emission in the NIR region were seen with adding H_2O_2. Moreover, an instantaneous hue shift was seen: under visible light, from red to yellow; under UV-365 nm, from pink to yellow. This result validates the development of a complex between probe 9 and H_2O_2. Based on spectroscopic data, the suggested mechanism showed that adding H_2O_2 to probe 9 caused the phenylboronic acid group from the probe's structure to cleave, hence increasing fluorescence emission. For the particular detection of H_2O_2 and viscosity in practical uses and living cells, Zhao-Min Lin and colleagues developed a FRET-based NIR fluorescent probe [59]. At 671 nm, the probe **10** displayed a red fluorescence signal which was ascribed to the FRET mechanism's suppression of the ICT process. After H_2O_2 is introduced, the red fluorescence signal at 671 nm gradually decreases while fluorescence emission at 550 nm is clearly detected. The suppression of the ICT process and the activation of the FRET mechanism explain this transformation. Without H_2O_2, two separate absorption peaks were seen in the absorbance probe 10 at 419 nm and 510 nm. After the addition, absorbance dropped at the absorption peak of 510 nm and showed a clear blue shift leading to the development of another peak at 419 nm. In both cases, a notable color shift was seen both before and after the addition of H_2O_2 with probe 10: from red to green under UV-365nm and from red to light yellow seen with the unaided eye. With rising H_2O_2 concentrations, the development in color change was essentially applied to strip paper testing. Moreover, all of these probes have been effectively used biologically on many cell lines. HepG2 cell line and zebrafish were used for Probe 8 evaluation in order to detect H_2O_2. Probe 8 showed red and yellow fluorescence emission both in and absent of H_2O_2. Strong red fluorescence in the NIR channel allowed Probe 9 to be applied to SW1783 cells for an endogenous detection of H_2O_2. But when H_2O_2 was added, the red emission in the NIR channel dropped greatly while the green channel showed a high fluorescence emission. Furthermore, probe 9 was used very well for the H_2O_2 detection among many food samples as seen in Figure 3. On pre-incubation, Probe 10 was treated with HeLa cells in the absence of TEMPO (H_2O_2 scavenger), therefore reducing fluorescence emission attributable to the removal of TEMPO by endogenous H_2O_2. The experiment was carried out under H_2O_2 presence, incubated with TEMPO and endogenous H_2O_2. The fluorescence intensity ratio seen throughout the red/green channel then changed as a consequence. The experimental data showed that probe 9 can identify both foreign and endogenous forms of H_2O_2.

 doi:10.20944/preprints202507.0403.v1

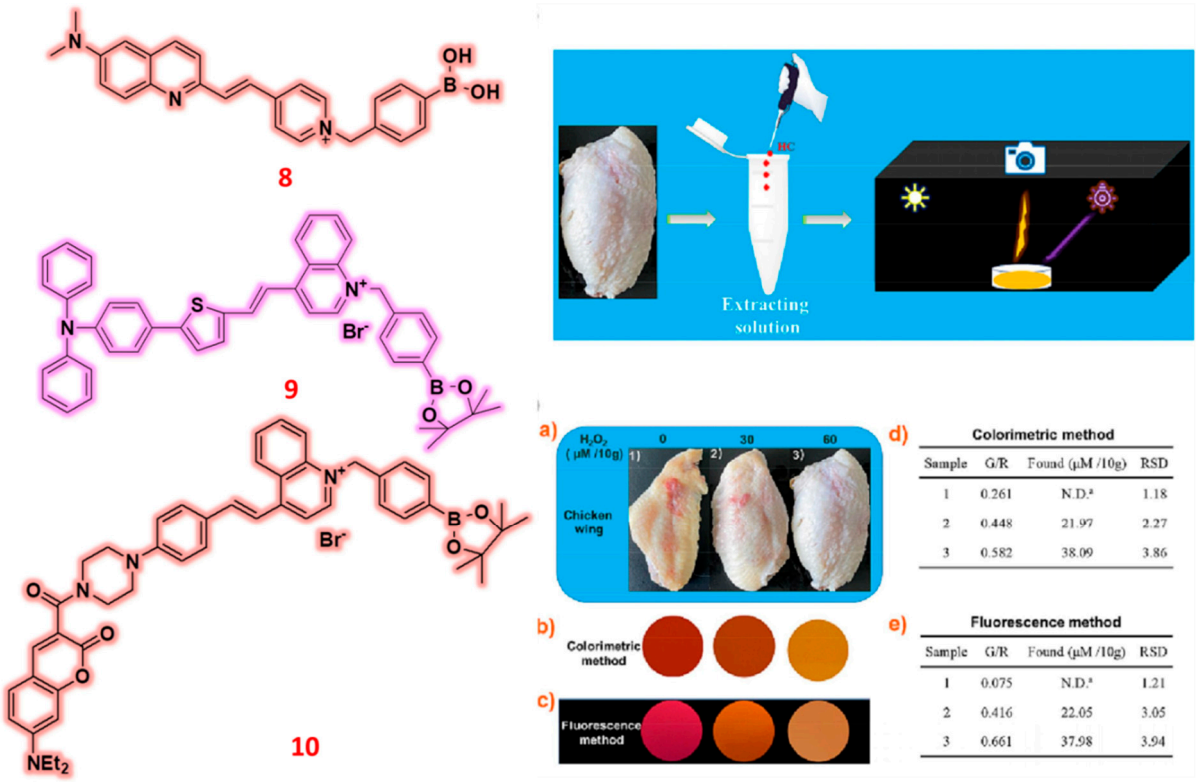

Figure 3. Structure of Quinoline based probes (**8-10**) for the detection of H_2O_2 ions and illustration of probe **9** for the sensing of H2O2 against different food samples. Reproduced with permission from Refs. [58], Copyright, Elsevier.

For the aim of monitoring H_2O_2 in diabetes, different cancer cell lines, and mouse models, the construction of quinolinium-based NIR fluorescent probe **11** was performed [60]. In investigations incorporating both absorption spectra and fluorescence spectra, the created probe 11 was treated with cations, anions, enzymes, and amino acids among other analytes. Probe 11 showed a significant absorption peak before different analytes were introduced. But the separate peak faded as the concentration of H_2O_2 rose, creating a new peak. Probe 11 showed modest fluorescence emission in the fluorimetric method under 725 nm of excitation wavelength. Fluorescence emission of the probe tested in isolation against the same analytes showed no variations. But adding H_2O_2 produced a slow rise in fluorescence intensity at 772 nm. Intramolecular charge transfer (ICT) mechanism causes the change in fluorescence emission. The ICT process was limited before H_2O_2 was developed, so fluorescence did not exist. But adding H_2O_2 caused the ICT process to be inhibited, which triggered fluorescence and increased fluorescence intensity. Probe 11 consists of a hydroxyl unit functioning as a fluorophore agent overall. This unit is released upon H_2O_2 addition, and strong fluorescence signal arises from borate ester group consumption. Wenbin Zeng and colleagues created a red-light emissive fluorescent probe using quinolinium as a fluorophore for the particular detection of hydrogen peroxide in live cells and rheumatoid arthritis. Successful characterization of the created probe **12** using colorimetric and fluorimetric titration approaches preceded its examination against different metal ions [61]. Original version of 12 showed absorption peak at 425 nm as an AIE probe. H_2O_2 caused this peak to vanish and a new absorption peak at 400 nm to arise. Probe 12 showed modest fluorescence emission in photoluminescence spectra ascribed to the central double bond. But when H_2O_2 was added, fluorescence emission was considerably increased, especially at 620 nm. The suggested mechanism is that a tetrahedral boronate intermediate results from H_2O_2 interacting with the electrophilic boron atom in the phenylboronate of the probe. Spectroscopic methods verifying the binding of H_2O_2 to probe 12 support this interaction even further. Using a new Aβ-targeted and blood-brain barrier (BBB)-permeable ratiometric H_2O_2-responsive fluorescence probe **13**, Hung-Wing

 doi:10.20944/preprints202507.0403.v1

Li and colleagues highlighted its application benefits in cellular and murine models of Alzheimer's disease [62]. At 388 nm, Probe 13 showed a wide absorption peak; at 574 nm, it had a modest emission peak. But the addition of H_2O_2 produced a red shift in the weak emission peak and the absorption peak to 485 nm and 661 nm correspondingly. Whereas the fluorescence intensity of the probe dropped at 574 nm in the fluorimetric titration method at an excitation wavelength of 490 nm, emission gradually rose at 661 nm. The production of the oxidized product came from 1,6-elimination via the methylphenyloxy linker in the phenolic intermediate increasing fluorescence emission. Furthermore, NMR and ESI-MS spectroscopic methods were used to confirm the oxidizing within the structure of the probe, therefore supporting the binding stoichiometry. Reportedly designed for selective administration to mitochondria, a fluorescent probe assigned as **14** showed extraordinary selectivity for H_2O_2 in brain tissue [63]. The probe 14 showed in the UV-visible spectra a clear absorption peak at 560 nm in water that changed to 590 nm in glycerol. Under fluorescence titration at 440 nm excitation wavelength, the fluorescence intensity showed a notable increase of around 120-fold at an emission wavelength of 670 nm. Colorimetric probe 14 showed an absorption peak at 420 nm when H_2O_2 was added; this is ascribed to the binding stoichiometry between probe 14 and H_2O_2. Adding H_2O_2 in fluorimetric analysis produced a notable increase in fluorescence intensity, by a factor of 80 from the first measurement. Following the addition of H_2O_2, the oxidation and hydrolysis processes in the probe's phenylboronic acid group produced changes in fluorescence intensity that later results in elimination via intramolecular rotation. Spectroscopic methods and DFT analysis tracked the reaction's development to show that H_2O_2 bound to the complexation of probe 14. Consistent use of confocal and fluorescent microscopy imaging methods allowed the remaining probes for biological studies to be done as shown in Figure 4. Examined against HeLa cell lines, probes 11 and 12 showed modest fluorescence emission in the red channel. Increasing amounts of H_2O_2 improved this emission. Using both non- and neuronal cell lines—more especially, N2a and N2aSW— Probe 13 was investigated. A notable fluorescence emission in the red channel came from increasing the H_2O_2 concentration. In cell imaging, the probe 14 experiment was carried out using SH-SY5Y human-derived neuroblastoma cell line. With yellow fluorescence, the probe showed modest emission; this effect changed with increasing H_2O_2 concentration. By use of a strong zone instead of weak yellow fluorescence emission, increasing the quantity of H_2O_2 confirmed the identification of H_2O_2. In a mouse model, the probes 13 and 14 were efficiently used to show a notable active fluorescence response following H_2O_2 injection in the pre-treated mouse model with probes 13 and 14.

 doi:10.20944/preprints202507.0403.v1

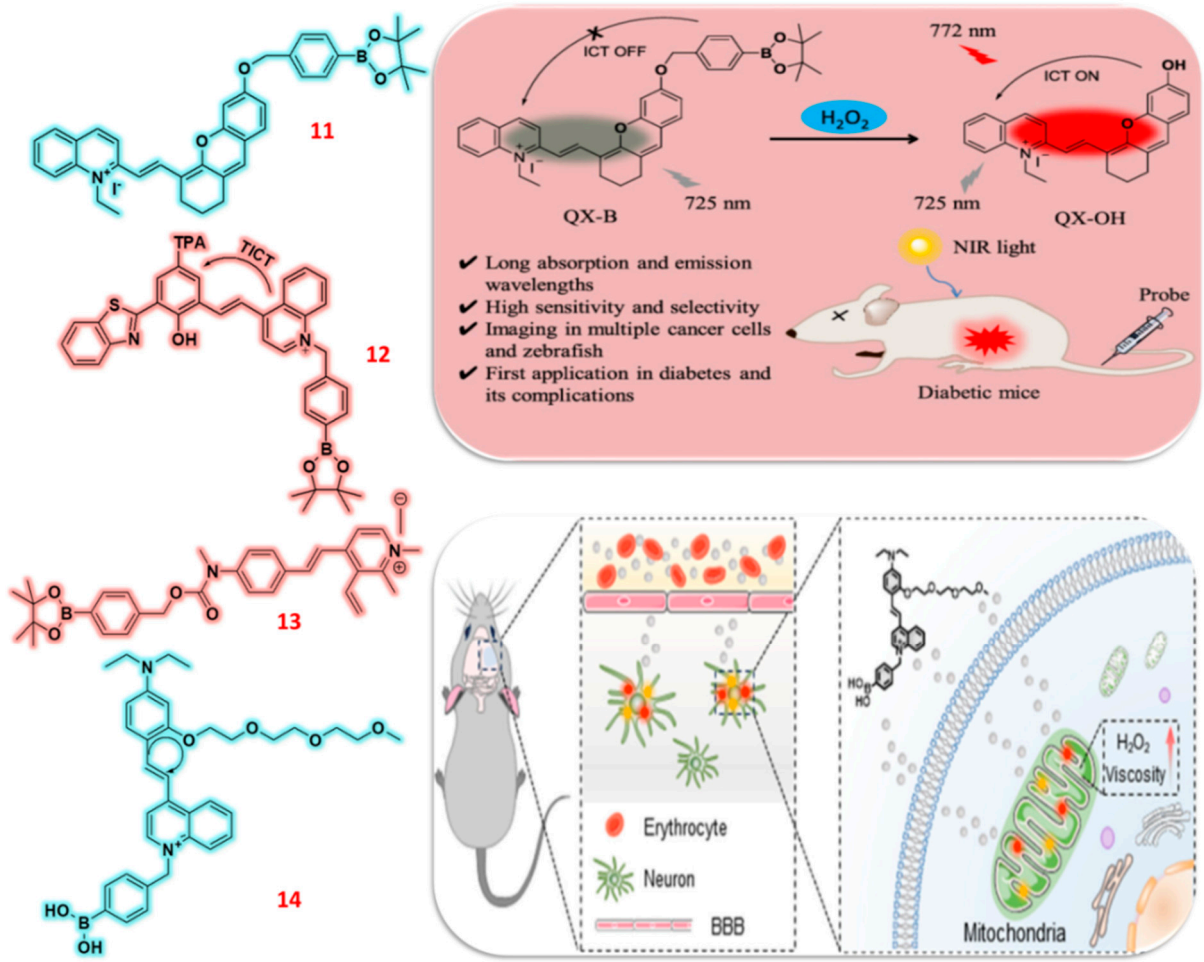

Figure 4. Structure of Quinolinium based probes (**11-14**) for the detection of H_2O_2 ions. Graphical illustration of long absorption and emission wavelength fluorescent probes **11** and **14** for its visualization in diabetic mice. Reproduced with permission from Refs. [60] [63], Copyright, American Chemical Society.

2.3. Pinocol Based Fluorescent Probes

Pinacol derivatives are essential in the development of probes, serving as adaptable functional handles and strong structural scaffolds. Their distinct characteristics enable the alteration of fluorophores, the addition of protecting groups, and the formation of bioconjugation linkers. Their role is crucial in the development of reactive oxygen species (ROS) probes, as they initiate a fluorescent signal upon cleavage by H_2O_2 or other ROS. Additionally, pinacol improves the stability and solubility of boronic acids during probe synthesis, thereby increasing their effectiveness. Pinacol-like diols demonstrate the capacity to bind analytes via boronic acid-diol interactions, which is beneficial for the accurate detection of glucose and fructose. The future of this field presents significant potential, incorporating two-photon probes for deep-tissue imaging, AIE probes for amyloid detection, and advanced metal complexation methods for hypoxia sensing. These derivatives, particularly boronate esters, play a vital role in the selective detection of reactive oxygen species (ROS) and other biological analytes. Their application significantly contributes to advancements in imaging technologies and improves our comprehension of intricate biological systems. To ensure low interference from other analytes, Tongsheng Chen and colleagues developed a near-infrared emitting ratiometric fluorescence probe intended for the selective detection of hydrogen peroxide [64]. The designed probe **15** proved to be very useful in cell imaging techniques for the detection of H_2O_2. First, the water-soluble ESIPT-based NIR fluorescent probe was tested using many analytes using both colorimetric and fluorimetric titration methods. The probe in colorimetric titration showed a significant absorption peak at 365 nm. But when H_2O_2 was added, the absorption

 doi:10.20944/preprints202507.0403.v1

peak at 365 nm shifted somewhat to 422 nm. In fluorimetry, without H_2O_2, excitation at a wavelength of 422 nm produced the probe displaying an enol emission at 538 nm. At 656 nm, we saw a notable red-shift in fluorescence emission. The observed red-shift in absorbance and fluorescence emission with H_2O_2 addition points to complex development. Furthermore seen was a color shift from colorless to yellow visually and from colorless to pink under UV-365 nm light with the addition of H_2O_2 to probe 15. Using an intracellular approach, a new NIR fluorescent probe **16** was designed for hydrogen peroxide detection and visualization [65]. Following the determination of the excitation wavelength, probe 16 was assessed under different cations, anions, and amino acid concentration. Attributed to the limitation of the intramolecular charge transfer (ICT), the probe showed mild fluorescence emission and no spectrum alterations together with other metal ions. H_2O_2 added to probe 16 produced a notable increase in fluorescence emission in the near-infrared spectrum along with a considerable Stokes shift of 122 nm. H_2O_2 added to the near-infrared emission produced a hydroxy group from the structure of the probe. To specifically detect H_2O_2 in melanoma, Guorui Li and colleagues created a dual locked NIR fluorescent probe using methylene blue. Cell lines and animals with tumours were used for application investigations [66]. Developed using methylene blue, probe **17** showed a turn-off fluorescence characteristic and modest fluorescence emission. Probe 17 shown absorption peak at 665 nm in colorimetric titration. It showed significant fluorescence in fluorimetric titration at 684 nm excitation wavelength. Probe 17 is used in combination with borate to detect H_2O_2, therefore enabling a turn-off to a turn-on fluorescence state. This procedure produces a 17-fold rise in fluorescence intensity following emission enhancement. The increase in emissions came from H_2O_2 transforming a non-fluorescent probe via cascade activation, hence activating the fluorescence signal from an "off" state to "on" one. As we seen in Figure 5, applications in both endogenous and exogenous cellular imaging, a new artificial intelligence fluorescent probe has been designed to see H_2O_2.

 doi:10.20944/preprints202507.0403.v1

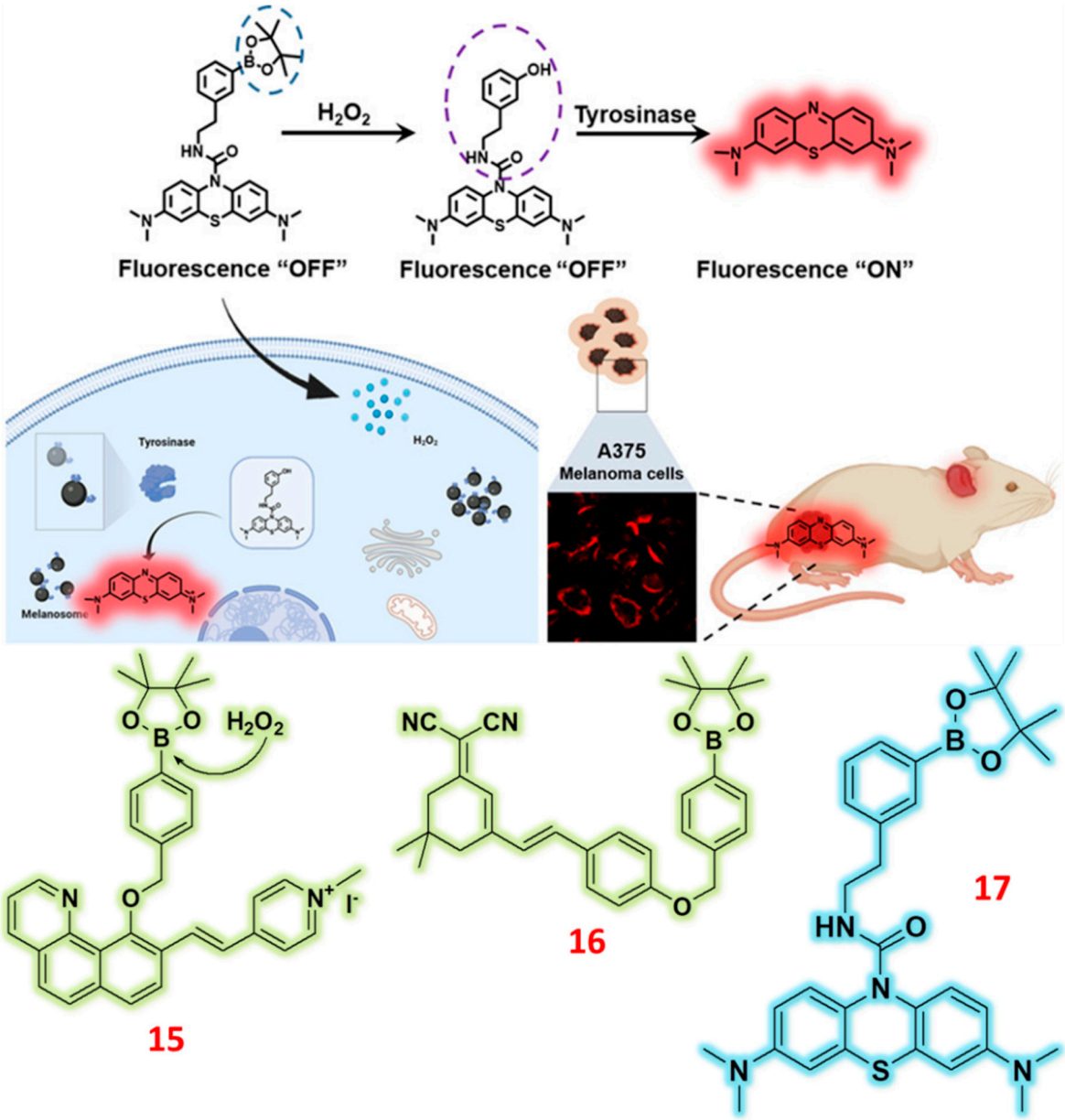

Figure 5. Structure of Pinocol based fluorescent probes (**15-17**) for the detection of H_2O_2 ions and illustration picture of probe **17** used for sensing in presence of H2O2 against A375 Melanoma cells in mice. Reproduced with permission from Refs. [66], Copyright, American Chemical Society.

Using imidazo pyridine conjugation, Junbing Jiang and colleagues created probe **18** that shows improved fluorescence for the detection of H_2O_2, hence reducing interference from other analytes [67]. Probe 18 shown low absorbance and fluorescence emission in both colorimetric and fluorimetric methods. But when stimulated at 500 nm, adding H_2O_2 produced a boost in fluorescence at 350 nm. Under UV-365nm light, a color change from blue to yellow was seen along with a matching slow rise in fluorescence intensity when the concentration of H_2O_2 was raised. The noted fluorescence increase and color shift demonstrate H_2O_2's binding recognition to probe 18. Designed and developed for the dual detection of H_2O_2 and HOCl, a bifunctional fluorescent probe designated as **19** Shunping Zang et al. Analyzed utilizing colorimetric and fluorimetric approaches for the detection of H_2O_2 and HOCl across two different channels, the bifunctional probe assigned number 19 showed two different absorption peaks [68]. Probe 19 showed an absorption peak at 480 nm; yet, a little red shift in the absorption peak was seen when H_2O_2 was added, ranging from 480 nm to 455 nm. Probe 19 showed weak fluorescence intensity in the absence of H_2O_2 when the excitation wavelength was set at 600 nm

 doi:10.20944/preprints202507.0403.v1

in the fluorimetric titration technique. On the other hand, in the presence of H_2O_2 the fluorescence emission showed an increase in intensity at 685 nm; other metal ions, in combination with probe 19, showed no changes in fluorescence intensity. Together with a little red shift in both methods, the addition of H_2O_2 causes changes in fluorescence emission and absorption, therefore indicating the development of a complex in red fluorescence. Particularly aiming at the detection of H_2O_2, the use of pinacol ester-based fluorescent probes was effectively carried out for cell imaging and biological uses. Treatments involving MCF-7 cells, HeLa cells, and RAW 264 cells applied probes 15, 16, and 19. In the experiment including seven cells and zebrafish for the H_2O_2 imaging, it was found that in the absence of H_2O_2, neither the red nor green channels showed emission. On the other hand, in the presence of H_2O_2, the red and green channels showed a great activity. While tumor-bearing mice were subjected to H_2O_2, pre-treatment for the probes 17 and 18 consisted of A375 cells and A549 cells. Strong fluorescence emission was shown by the cell lines pre-treated with probes 17 and 18; correspondingly, probe 17 displayed red channel fluorescence and probe 18 displayed green channel fluorescence (Figure 6).

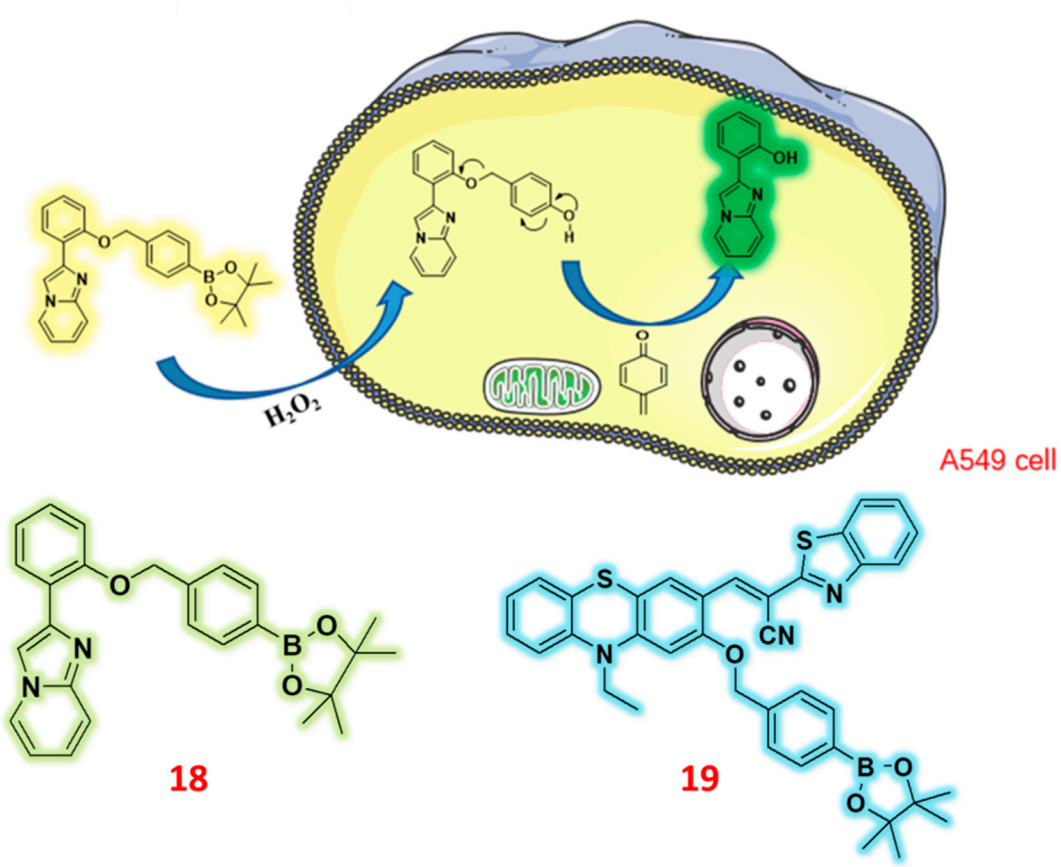

Figure 6. Structure of Pinocol based fluorescent probes (**18 & 19**) for the sensing of H_2O_2 ions and graphical construction of probe **18** used for sensing in presence of H_2O_2 against A549 cell line. Reproduced with permission from Refs. [67], Copyright, MDPI.

2.4. Aldehyde Based Fluorescent Probes

Because of their great reactivity and broad range of use, Aldehyde-based fluorescent probes are very vital in chemical and biological research. These probes have great reactivity thanks to aldehyde groups (–CHO), which may be exactly changed to recognize a wide spectrum of analytes including thiols, Reactive Oxygen Species (ROS), Reactive Nitrogen Species (RNS), and amines/amino acids. In response to specific target molecules, these sophisticated fluorescent probes show amazing capacity to either activate (turn-on) or deactivate (turn-off) fluorescence. This special ability helps scientists to

 doi:10.20944/preprints202507.0403.v1

precisely monitor biological events. In fields like biochemistry, medicine, and environmental research, aldehyde-based fluorescence probes have become indispensable tools. Their great selectivity, sensitivity, and adaptability make them useful instruments for the detection of important analytes and help to reduce interference. Moreover, their ability to provide real-time, non-invasive imaging sets them as essential instruments in the development of our knowledge of disease processes and the enhancement of diagnostic capability. By means of these probes, scientists may get important insights that propel development in fundamental science and clinical applications, hence generating major discoveries in health and environmental sustainability. Kehua Xu and associates have created a new mitochondria-targeting NIR fluorescent probe **20** to clarify how H_2O_2 and other metal ions affect viscosity interactions [69]. Under low viscosity, the probe 20 displayed modest fluorescence emission because to molecular rotation. On high viscosity, on the other hand, the molecular rotor is hindered and probes 20 exhibits intense fluorescence emission. Using an excitation wavelength of 685 nm, the fluorimetric titration technique for probe 20 was assessed with respect to other metal ions and H_2O_2. Under low viscosity circumstances, the molecular rotor showed mild fluorescence emission; this was improved upon H_2O_2 addition. H_2O_2 produced the probe 20 with high fluorescence emission, which is characterized by an intensity rise. Still, too strong metal ions might cause viscosity to drop. The state of probe 20 concerning viscosity shows the stability of the probe under different circumstances. Furthermore, probe 20 might be a useful fluorescent agent for observing changes in mitochondrial viscosity in physiological surroundings. Designed for use in cell imaging and food sample monitoring of HSO_3^- and H_2O_2, a reversible near-infrared fluorescent probe under designation **21** was created. Qingtao Meng and colleagues created a probe with a D–π–A–π–D conjugating structure combining a benzopyrylium moiety with a C=C double bond [70]. First testing the probe 21 used cations, anions, and amino acids among other analytes. The findings showed that in contrast to other metal ions, the probe specifically picks up HSO_3^- ions. Probe 21 detects HSO_3^- ions only in absorbance spectra, displaying a red-shift-oriented new absorption peak. Moreover, the Michael addition process disturbs the link between the C=C double bond and the benzopyrylium moiety, therefore progressively reducing another absorption peak at 605 nm. In fluorimetry, probe 21 detects HSO_3^- ions by noting a decrease in fluorescence intensity, ascribed to quenching of fluorescence emission with respect to other metal ions. Variations in the probe's moiety after HSO_3^-) introduced explained the variations in absorbance and emission. Visually, one also saw a hue shift from blue to colorless. Sequential sensing of H_2O_2 using the complexation of probe 21 with HSO_3^- resulted in the fascinating recovery of the spectroscopic characteristics of probe 21. The main absorption peak at 605 nm shows a rise in concentration of H_2O_2; the peak almost returns to its former location. Noted with increasing H_2O_2 concentration during complexation, the observed color shift moves from colorless to blue. This obviously shows that the recycling procedure may help to recover the spectroscopic characteristics of probe 21 in the presence of H_2O_2. Developed for selective sensitivity to ROS/RNS and base ions, a dual responsive NIR-II fluorescent probe **22** may be rather important in biosensing applications [71]. Development and efficient usage of the NIR-II probe for biosensing purposes in a mouse model to track cystitis and colitis under different pH levels and time intervals is discussed (Figure 7). Evaluated with many analytes, the produced probe 22 showed emission in the NIR-II spectrum. The probe showed an absorption peak at 870 nm; treatment with H_2O_2 produced a red shift of the absorption peak. Probe 22 shown mild fluorescence emission in fluorimetric titration. From 0 to 500 μM, a rise in the concentration of H_2O_2 produced a slow increase in fluorescence intensity accompanied by a little red shift from its natural location. The limit of the intramolecular charge transfer (ICT) mechanism before the introduction of H_2O_2 explained the sudden changes in absorbance and emission. The hydroxyl group was eliminated upon H_2O_2 addition, producing a phenolic fluorophore effect displaying the ICT process. Designed for the evaluation of the effectiveness of photodynamic and photothermal synergistic treatment in cell imaging applications, Chun- Yan Li and the research team have developed a dual activated NIR-I/NIR-II fluorescent probe. Designed and constructed, the probe **23** showed a mild fluorescence effect, hence absenting photodynamic treatment (PDT) and photothermal therapy (PTT) [72]. The probe 23 was investigated

 doi:10.20944/preprints202507.0403.v1

both in the presence and absence of H_2O_2 with viscosity changes meant to improve the fluorescence effect. Under high viscosity, the probe showed two absorption peaks in colorimetric analysis at 725 nm and 798 nm. On the other hand, the absorption peaks were strengthened when high viscosity was maintained in the presence of H_2O_2. Under high viscosity, probe 23 shown no fluorescence response at wavelengths of 810 and 945 nm in the fluorimetry study. Under the same high viscosity circumstances, however, the addition of H_2O_2 produced a notable fluorescence response marked by a fluorescence intensity increase. Further confirming that probe 23, which showed weak fluorescence, may be triggered only in the presence of H_2O_2 under circumstances of high viscosity, are the studies using colorimetric and fluorimetric approaches. Selective detection of H_2O_2 utilizing both colorimetric and fluorimetric techniques made use of another AIE fluorescent probe. Its use was shown using live tumor cells and in-vivo experiments [73].

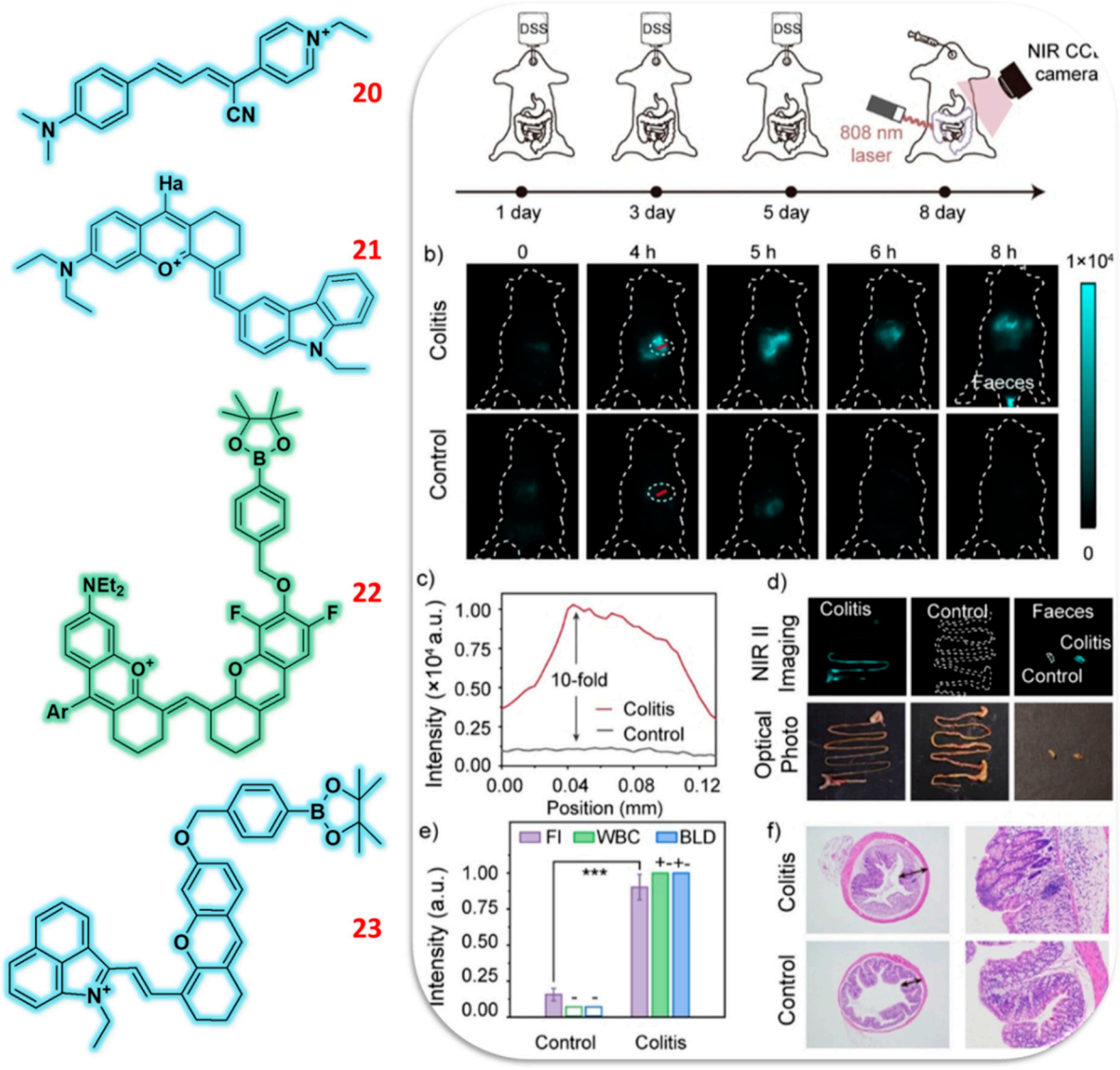

Figure 7. Structure of Aldehyde based fluorescent probes (**20-23**) for the selective detection of H_2O_2 ions and In vivo monitoring of colitis with probe **22** with its schematic illustration of cystitis mice model and the application of **22** for colitis monitoring. Reproduced with permission from Refs. [71], Copyright, Wiley.

Originally combined as a solution comprising probe **24** and H_2O_2, the produced probe showed a significant peak at 430 nm. But a new strong absorption peak with a little blue shift at 450 nm emerged during incubation with H_2O_2. Probe 24, which included H_2O_2, first showed quenched fluorescence emission after the excitation wavelength for fluorimetric titration being adjusted at 450

 doi:10.20944/preprints202507.0403.v1

nm. After adding H_2O_2 during incubation, this emission was then strengthened and shown great fluorescence at 630 nm. The addition of H_2O_2 to the probe 24 + H_2O_2 combination split the borate moiety from the probe, therefore producing changes in emission and absorbance. This mechanism enabled the AIE fluorophore to be released, hence increasing fluorescence intensity and fluorescence activation. Designed for dual detection of SO_2 and H_2O_2 in conditions characterized by low polarity and high viscosity, Jun Ai and colleagues have developed a flexible fluorescent probe **25** [74]. Attractive near-infrared characteristics for polarity, viscosity, and SO_2/ H_2O_2 levels allowed the probe 25 to show a clear fluorescence emission peak at 705 nm. Probe 25 showed highest absorption in the absorbance spectra at 648 nm, which matched the excitation wavelength of 648 nm. With a progressive concentration, the fluorescence emission at 705 nm showed a notable drop in fluorescence intensity. On the other hand, the fluorescence intensity at 705 nm emission also showed rise when viscosity rose progressively. SO_2 produced a decrease in the absorption peak at 648 nm and the emission peak at 710 nm when testing probe 25 with SO_2/ H_2O_2. Sequential sensing in the presence of H_2O_2 restored both the absorption peak and emission peak to their natural forms. Further evidence of complicated development came from the color change from blue to colorless in the presence of SO_2 reversing from colorless back to blue in the presence of H_2O_2. An uncontrolled intramolecular charge transfer (ICT) activity in probe 25 explains the observed variations in absorbance and emission. Under low polarity and high viscosity especially, the twisted intramolecular charge transfer (TICT) mechanism completely reduced this activity in presence of SO_2/ H_2O_2. Using a similar approach considering polarity and viscosity parameters, a second NIR fluorescent probe **26** was developed specifically for the detection of H_2O_2 across different cell lines [75] (Figure 8). Under high viscosity, the probe in a free condition showed a pronounced absorption peak at 585 nm, which was much rose at the same wavelength. High viscosity conditions in fluorimetry produced a notable increase in fluorescence emission at 750 nm along with a considerable Stokes shift of 165 nm. Unlike polarity, the fluorescence emission of probe 26 was much reduced by an 82-fold. After polarity and viscosity experiments, probe 26 was assessed in both colorimetric and fluorimetric environments in presence of H_2O_2. Probe 26 showed a clear absorption peak at 560 nm, which then reduced following the addition of H_2O_2 to produce a new absorption peak at 405 nm. In fluorimetry, probe 26 first showed faint emission. H_2O_2 added raised the fluorescence intensity by a factor of 20 at 650 nm. Moreover, the addition of H_2O_2 to probe 26 clearly changed the color from purple to yellow, suggesting the development of a complex. The discussed probes here were successfully utilized for the detection of H_2O_2 under different viscosity and polarity against HepG2 cells (20), Zebra and mouse (21), mice (22), HeLa cells and tumor bearing mice (23), 4T1 cells and 4T1 bearing mice (24), HeLa and CT26 cell lines (25) and 4T1 cells and mice model (26).

 doi:10.20944/preprints202507.0403.v1

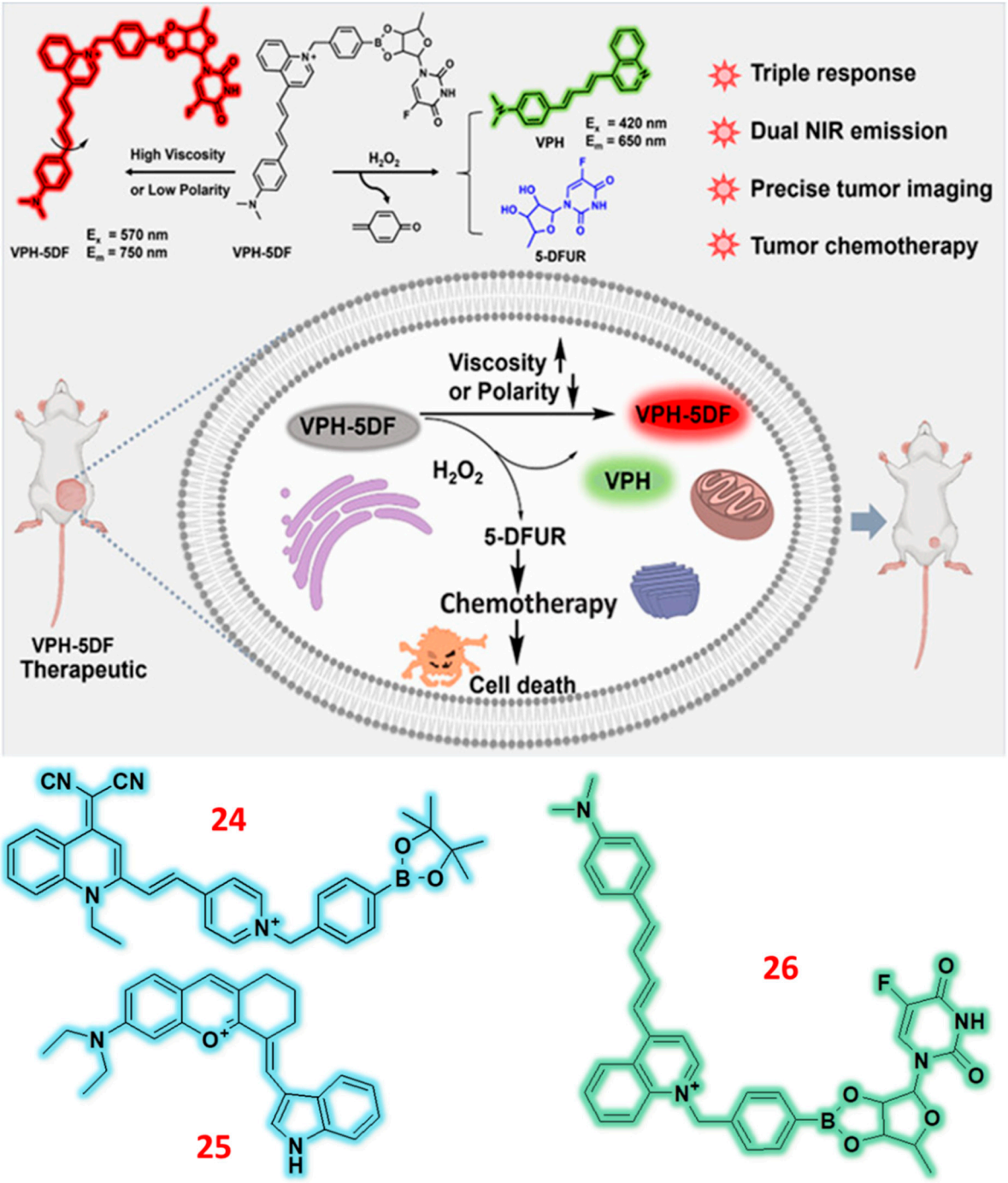

Figure 8. Structure of Aldehyde based fluorescent probes (**24-26**) for the specific detection of H_2O_2 ions and graphical illustration of probe **26** in presence of H2O2 for visualization detection in VPH-5DF mice model. Reproduced with permission from Refs. [75], Copyright, American Chemical Society.

2.5. Hemicyanine Based Fluorescent Probes

Because of its amazing characteristics—including improved quantum yields and configurable spectrum features fluorescent probes based on hemicyanine are becoming more and more common in scientific teaching and research. Their near-infrared (NIR) spectrum of absorption and emission greatly increases their relevance in disciplines like bioimaging, medical diagnostics, and real-time biomolecule identification. High-resolution imaging in complicated biological contexts depends on the probes penetrating deeply into biological tissues and simultaneously maintaining a suitable signal-to----noise ratio. Recent developments in hemicyanine dyes have produced imaging probes intended especially for targeting mitochondria. The probes show better endurance and increased

 doi:10.20944/preprints202507.0403.v1

fluorescence qualities. Currently, research efforts concentrate on improving these probes to maximize their biocompatibility and solve any limits for in vivo uses. Designed for the imaging and detection of H_2O_2 in many disease types, including lung, liver, and cancers, a flexible NIR fluorescent probe **27** was created [76] (Figure 9). Weak absorption and emission in the NIR range were ascribed to the limitation of the intramolecular charge transfer (ICT) mechanism within the probe, hence quenching of fluorescence. Apart from a lesser absorption peak at 698 nm, the probe 27 showed two clear absorption peaks at 546 nm and 576 nm. The absorbance of the peaks at 546 nm and 576 nm dropped as the quantity of H_2O_2 rose; the absorbance at 698 nm rose dramatically. Probe 27 was tuned in fluorimetric titration at 698 nm. Along with a color shift from purple to light blue, the probe showed modest emission at 720 nm that considerably increased with increasing H_2O_2 concentration from 0 to 500 μM. The uncontrolled intramolecular charge transfer activity, which triggered the fluorescence, changed absorbance and emission with the addition of H_2O_2. Designed for the particular detection of H_2O_2, a fluorescent probe **28** shows a fast and selective response in detecting H_2O_2 within active tumor cells [77]. Under the presence and absence of H_2O_2, the photophysical response of probe 28 was evaluated using UV-visible absorption and fluorescence spectroscopy. Under UV-visible spectrum analysis, probe 28 showed a large absorption peak at 584 nm. H_2O_2 caused this peak to move to 681 nm and a color change from violet to blue. Probe 28 showed little fluorescence emission in fluorimetric titration spectra when stimulated at 702 nm. With increasing H_2O_2 concentration, this emission was much raised, almost 25-fold. The complexation solution was incubated under many biomolecules both in presence and absence. The findings showed that the other biomolecules did not interfere with the complexation, therefore verifying the relevance of probe 28 for biological uses in the selective detection of H_2O_2. Aimed at monitoring in plants, Na Niu and colleagues developed a new NIR fluorescent probe for the particular detection of H_2O_2 [78]. Examined under many biomolecules in combination with H_2O_2 at an excitation wavelength of 650 nm, the built probe **29** showed 29 was treated with H_2O_2 both in and without of the reagent as an NIR probe. Excitation at 650 nm produced modest emission at 720 nm in the absence of H_2O_2; this was much improved with the addition of H_2O_2. Probe 29 was assessed in the presence of H_2O_2 throughout a pH range of 3 to 10 in order to improve the fluorescence intensity even further. Still, the probe showed no change in emission in both acidic and basic environments. Probe 29 showed a slow rise in fluorescence intensity under neutral and alkaline conditions in the presence of H_2O_2 along with a little red shift in emission ascribed to the intramolecular charge transfer (ICT) mechanism. Combining a boronic acid ester as a recognition site for hydrogen peroxide (H_2O_2) and biotin as a tumor identification site. Probe 27 first was used for the H_2O_2 detection on HeLa cells as well as liver, lung, and animal models. Probe 28 then was used to mouse tumor tissue and A49 cells. Analyzed utilizing many plant components, including leaves and onions, Probe 29 showed a high red emission in response to fluorescence imaging detection of H_2O_2.

 doi:10.20944/preprints202507.0403.v1

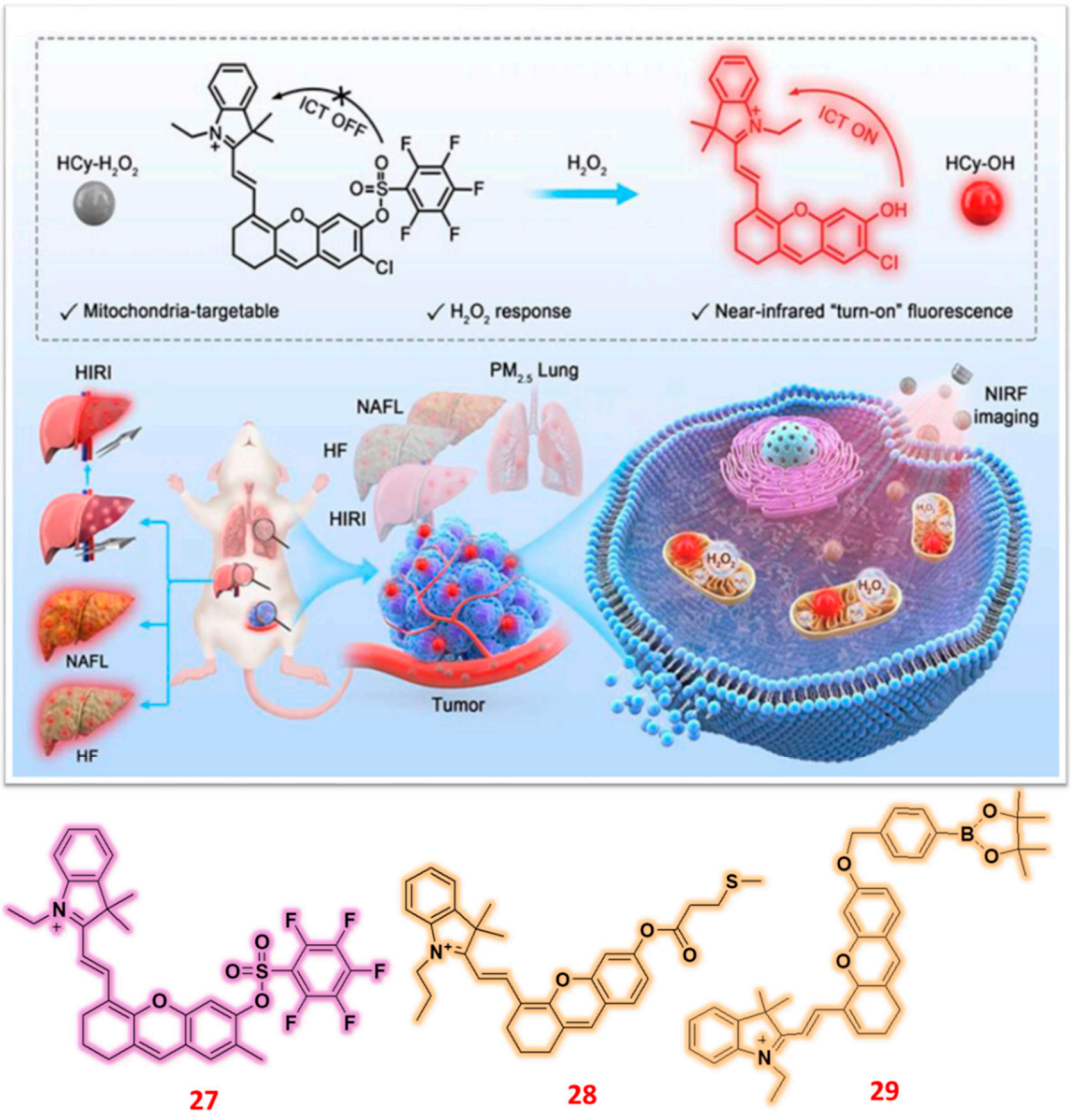

Figure 9. Structure of Hemicyanine based NIR fluorescent probe (**27-29**) for the sensing of H_2O_2 ions and probe **27**′s application against tumor bearing mice model. Reproduced with permission from Refs. [76], Copyright, American Chemical Society.

Hong Liu and colleagues created a near-infrared fluorescence probe This probe may increase fluorescence emission in reaction to H_2O_2 presence [79]. In in vivo applications, the created probe **30** was used quite well to detect H_2O_2. Using absorbance and emission spectroscopic analyses, Probe 30 was investigated both in presence and absence of H_2O_2. The probe in its natural form had a significant absorption peak at 544 nm in UV-visible spectra. But when H_2O_2 was present, the absorption peak shifted from 544 nm to 680 nm and the hue changed from purple to blue. Fixing the excitation wavelength for fluorimetric titration, the feeble emission of the probe at 707 nm showed a slow rise in intensity with increasing H_2O_2 concentration. As the concentration of H_2O_2 was raised gradually from 0 to 100 μM, the emission changed. Especially, fluorescence intensity increased significantly at a dosage of 50 μM. The interaction between the boronic acid ester group and H_2O_2 explains this rise in fluorescence emission in the near-infrared (NIR) region. The complicatedation of probe 30 with H_2O_2 was assessed with respect to other reactive oxygen species (ROS) molecules concurrently. There was no change in fluorescence intensity, hence it is clear that probe 30 might be rather important for the selective detection of H_2O_2 in practical uses. For the intended imaging of mitochondrial H_2O_2 in the presence of viscosity, Yang Liu and colleagues have developed a dual-modal probe, NIRF/PA [80]. Apart from in vivo and in vitro uses aiming at targeting mitochondria and imaging changed

 doi:10.20944/preprints202507.0403.v1

H_2O_2 levels and viscosity inside cells, the developed probe **31** was efficiently used for the diagnosis of PD. First used in absorbance spectra, the special probe 31 showed a significant absorption peak at 710 nm. A little change in fluorescence intensity was seen when the excitation wavelength was set at 725 nm and the concentration was raised from 0 to 200 μM. The probe was then tested against glycerol at different concentrations ranging from 0 to 90%, where a significant increase in intensity was seen. Examined under many situations, Probe 31 included glycerol and H_2O_2 both present and absent. A modest increase in emission and absorption was seen in the presence of H_2O_2/glycerol. On the other hand, simultaneous application of H_2O_2/glycerol clearly increased fluorescence intensity and absorbance. Other analytes then were investigated under the H_2O_2/glycerol system, where no interference from other analytes was noted. Under the presence of H_2O_2, the borate unit in probe 31 experienced an oxidative elimination process that restored fluorescence. DFT, FT-IR, and ESI-MS spectroscopic methods were used to verify the complexation system and prove the oxidative elimination process took place within the probe. Using colorimetric and fluorimetric techniques, Bo Tang and colleagues developed Probe **32** for the particular detection of H_2O_2 and viscosity [81]. For in situ H_2O_2 detection as well as in vivo viscosity biological uses, the probe 32 proved really useful. Probe 32 was tested first using many analytes. Whereas the other analytes did not show any further spectrum changes, the addition of H_2O_2 changed absorbance and fluorescence emission. Applying the same method, the probe's viscosity response was assessed. It was seen that the absorbance and emission of probe 32 likewise rose when the viscosity concentration rose. Structural alterations cause a slow reduction in fluorescence emission when H_2O_2 is added to the 32+viscosity system. In low viscosity, however, probe 32's fluorescence emission is modest; so, under high viscosity circumstances, it recovers to its natural form. The spectrum investigations demonstrate that probe 32 is able to detect viscosity and H_2O_2 selectively in biological applications spanning many excitation wavelengths. For the detection of H_2O_2 in different cancer cell lines and mice models, all under mentioned probes were efficiently used. While probe 31 was assessed using SH-SY5Y cells and Drosophila culture (Figure 10), where it demonstrated high red fluorescence emission, probe 30 underwent successful testing with 4T1 cells and a 4T1 tumor-bearing animal model. In tests involving mice and foam cells, Probe 32 was used to identify H_2O_2 via confocal fluorescence imaging.

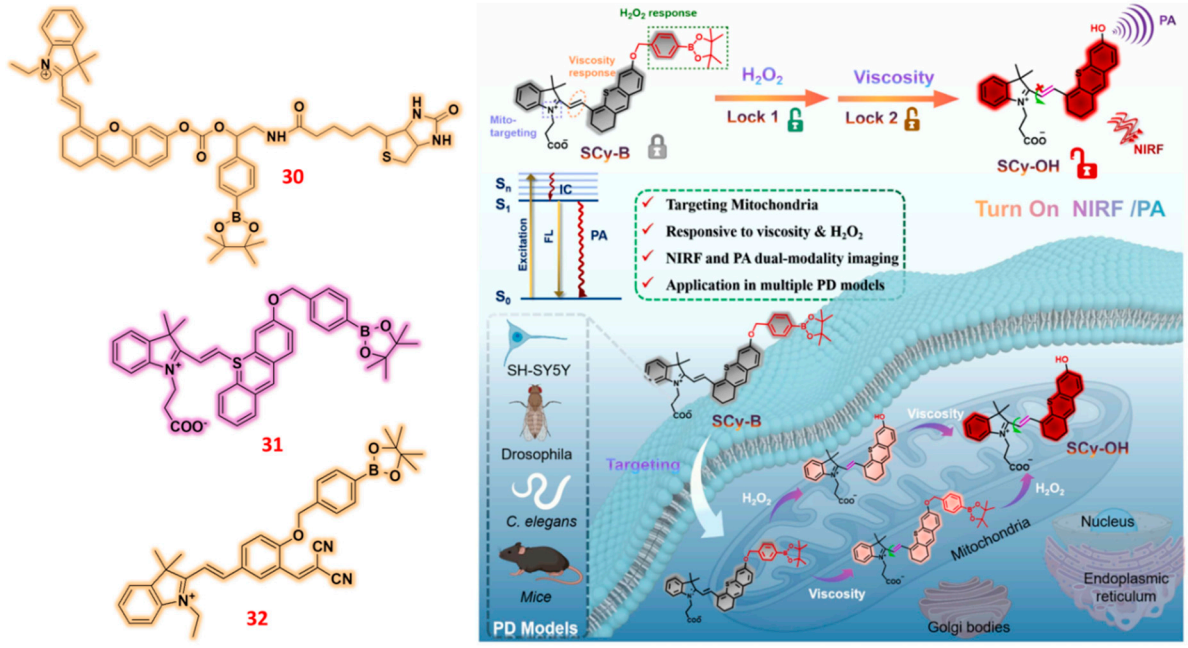

Figure 10. Structure of Hemicyanine based NIR fluorescent probe (**30-32**) for the sensing of H_2O_2 ions and probe **31**'s application for the detection of H_2O_2 against PD bearing mice model and SH-SY5Y bearing drosophila. Reproduced with permission from Refs. [80], Copyright, Elsevier.

 doi:10.20944/preprints202507.0403.v1

2.6. Isophorone Based Fluorescent Probes

As the field of chemical and biological sensing continues to advance, the examination of fluorescent probes based on isophorones has become an extremely significant area of study. It's possible that this transformation is connected to the vast range of applications that these probes have, in addition to the excellent photophysical properties that they possess. It is possible to give an inherent value to fluorescent probes due to the fact that they emit light, are sensitive to changes in the environment, and have outstanding versatility in applications linked to chemical and biological sensing. The capability of these technologies to deliver high-contrast imaging in real time positions them as key instruments in a number of different fields, including biology, environmental monitoring, and materials research, among others. It seems from this that there is potential for significant advancements in both research and application. Using dicyanoisophorone and dicyanomethylene derivatives for the particular detection of H_2O_2, three different research groups have created and produced NIR-based fluorescent probes **33** [82], **34** (i), **34** (ii) [83], and **35** (i), **35** (ii) [84]. Every probe has been used successfully in a biological context. Probe 33 was first checked under many analytes. Red shift-driven notable changes in absorbance and fluorescence emission were seen with the addition of H_2O_2. The removal of the phenyl boronate group in the fluorophore caused the variations in fluorescence absorption and emission; this increases fluorescence intensity in the near-infrared range. Treating Probes 34 (i) and 34 (ii) with H_2O_2 during a 0 to 240 minute period resulted in Whereas probe 34 (ii) finished the procedure in 87 minutes, showing a quicker reaction than probe 34 (i), probe 34 (i) needed 240 minutes for the treatment. Examined in the presence of H_2O_2 throughout a range of concentrations from 0 to 100 equivalents was Probe 34 (ii). With an excitation wavelength set at 550 nm, the data revealed a slow rise in fluorescence intensity at 645 nm. Examining probe 34 (ii) behaviors in the presence and absence of other metal ions alongside H_2O_2 allowed one to assess interference from other analytes. The findings showed that during the complexation of probe 34 (ii) with H_2O_2 no interference from other metal ions took place. The addition of H_2O_2 caused the changes shown in the emission spectra; this helped the borate group to cleave off the fluorophore, hence improving the fluorescence intensity. The probe showed an ICT process limitation before the addition of H_2O_2, which was then inhibited after the reaction with H_2O_2. Using dicyanomethylene, two NIR fluorescent probes—35(i) and 35(ii)—have been created for the particular detection of H_2O_2 across many cell lines and in mice within the NIR range. Prior to and during the addition of H_2O_2, photophysical tests of the probes were performed using both colorimetric and fluorimetric methods. Along with absorption peaks at 410 nm and 413 nm before the addition of H_2O_2, the probes 35(i) displayed modest emission at wavelengths of 653 nm and 655 nm. Under H_2O_2, a slow rise in fluorescence emission was seen along with a significant absorption peak cantered at 410 and 412 nm. The fluorescence emission at 653 nm showed a slow rise in intensity when one raised the concentration of H_2O_2 from 0 to 100 μM. Tested against many analytes, the complexation technique showed no interference from other analytes—which would be important for biological uses. As well as MCF-7, MCF-10A, DU-145 cells, and tumor-bearing mice for probes 35(i) and 35(ii), the dicyanoisophorone and dicyanomethylene based probes presented in this discussion were essentially used for the detection of H_2O_2 across various cell lines, including HepG2 cells, zebrafish, and inflammatory mice models for probe 33; HeLa cells and zebrafish for probes 34(i) and 34(ii). The probes showed mild fluorescence emission across many channels; nevertheless, the addition of H_2O_2 produced significant fluorescence emission in the red channel (Figure 11).

 doi:10.20944/preprints202507.0403.v1

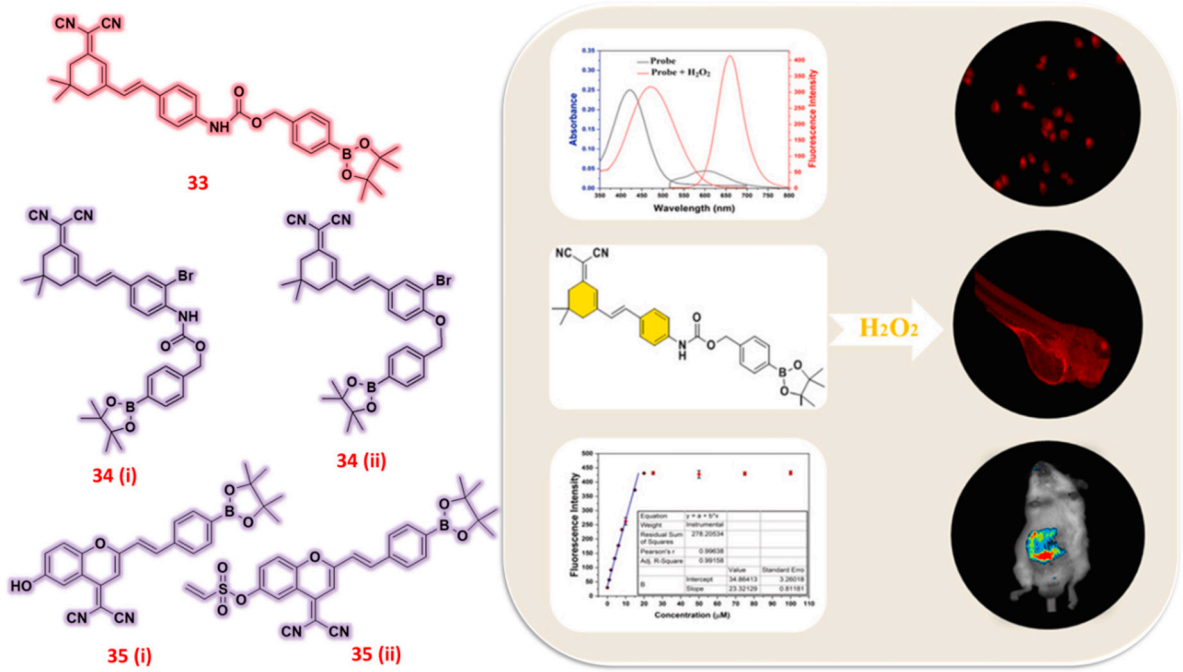

Figure 11. Structure of Isophorone based fluorescent probes (**33-35**) for the detection of H_2O_2 ions and cell imaging application of probe **33** in presence of H2O2 against HeLa cells, zebra fish and mice model Reproduced with permission from Refs. [82], Copyright, Elsevier.

2.7. Indole Based Fluorescent Probes

Indole derivatives are key components of fluorescent probes due to their photophysical properties, structural flexibility, and ability to interact with a wide range of analytes. These precise probes are essential for detecting metal ions, anions, ROS/RNS, pH alterations, biomolecules, and cellular microenvironments. Indole derivatives are effective in identifying and quantifying analytes due to their strong fluorescence emission and high quantum yields. Many indole derivatives exhibit a large Stokes shift, reducing self-quenchishing and improving signal-to-noise ratio. This trait is crucial for reliable detection in complex environments with interference. Indole derivatives employ Intramolecular Charge Transfer (ICT) and Photoinduced Electron Transfer (PET) to detect metal ions, anions, and reactive species (ROS/RNS). The techniques increase sensitivity and specificity, allowing precise measurement of trace analyte levels. Indole-based fluorescent probes are useful for biological monitoring of biomolecules, cellular processes, and physiological conditions. Biosensing technologies and medical diagnostics have evolved due to contributions, allowing inventive healthcare methods. Fluorescence probes need indole derivatives' particular properties and versatility, enabling substantial advances in many scientific fields and valuable applications. Based on indole, three independent research teams have produced three different NIR-I/II fluorescent probes for the particular detection of H_2O_2 using spectroscopic investigations. Crucially for cell imaging research, Hu Xiong et al. created an NIR-II fluorescent probe **36** with great selectivity and sensitivity towards H_2O_2, thereby enabling a change in fluorescence emission from turn-off to turn-on [85]. Analyzed in its present state, Probe 36 showed an absorption peak at 525 nm and a faint emission at 990 nm, ascribed to the development of an acceptor-π-acceptor (A-π-A) system. From 0 to 250 μM, the addition of H_2O_2 causes variations in absorbance and emission. Whereas another absorption peak at 790 nm indicated a rise in colorimetric analysis, the absorption peak at 525 nm showed a decline. By contrast, the fluorimetric study found a notable Stokes shift of 200 nm and a marked increase in the fluorescence emission peak at 990 nm. The modifications were ascribed to the inclusion of H_2O_2, which experiences structural rearrangement in concert with a donor-π-acceptor (D-π-A) system, hence generating NIR-II fluorescence emission via an ICT process. David G. Churchill and colleagues created a highly selective NIR fluorescent probe called **37** for sensitive

 doi:10.20944/preprints202507.0403.v1

detection of H_2O_2 in the presence of several ROS and RNS analytes by use of an ICT sensing system [86]. Without analytes, the probe 37 in a free form was investigated and showed a significant absorption peak at 527 nm that changed to 552 nm following H_2O_2 addition. Furthermore, the free-state probe 37 showed modest fluorescence emission at 617 nm with the excitation wavelength set at 552 nm; this effect grew with increasing H_2O_2 concentration from 0 to 18 equivalents. No interference was seen in the complexation state of probe 37 with H_2O_2; during complexation, the presence of certain reactive oxygen species (ROS) and reactive nitrogen species (RNS) analytes did not produce any changes in emission. The presence of H_2O_2, which serves as an electron receptor and helps the ICT process from the indole nitrogen donor inside the probe structure to the malononitrile ring, was responsible for the noted variations in emission and absorbance measurements. For the particular detection of hydrogen peroxide (H_2O_2) in tumor targeted uses for cell imaging, Wancun Zhang and colleagues created a new near-infrared fluorescent probe using indole derivatives [87]. Two absorption peaks at 600 nm and 660 nm on the produced probe **38** showed a significant change from 600 nm to 686 nm following H_2O_2 injection. Probe 38 showed a modest fluorescence signal in its natural form at 710 nm in the emission spectra. Nevertheless, the fluorescence emission at 710 nm exhibited a slow rise in intensity when the concentration of H_2O_2 was raised from 0 to 100 μM, culminating at 100 μM. The suppression of the ICT process caused by the replacement of the phenyl borate ester group with the hydroxyl group of the probe produced the emission and absorbance seen before the addition of H_2O_2. H_2O_2 brought about changes in absorbance and an increase in emission. The cleavage of the phenyl borate group is responsible for this alteration as it generates a strong NIR fluorescence signal by releasing a hydroxyl group. Strong fluorescence emission in the presence of H_2O_2, which was essentially used for the detection of H_2O_2 in biological applications, shown by the probes produced from indole derivatives. Using an APAP-induced liver damage mice model and a HeLa cell line, the probe 36 was assessed to detect H_2O_2 using fluorescent NIR-II imaging method (Figure 12). Pre-incubated under probe 36, the cells and mouse model were investigated both with and without H_2O_2. Imaging showed little emission in the absence of H_2O_2; significant NIR-II fluorescence signals were seen in the presence of H_2O_2. Under the same technique, a further probe assigned number 37 was tested against the lung cancer cell line (A459 type) and zebrafish. Using H_2O_2 produced a strong fluorescence signal seen in the red emission channel across both models. Examined in both presence and absence of H_2O_2 inside the 4T1 cell line at different concentrations was probe 38. H_2O_2 caused a significant fluorescence signal in the red emission channel. NAC addition helped the fluorescence signal to return to its natural condition.

 doi:10.20944/preprints202507.0403.v1

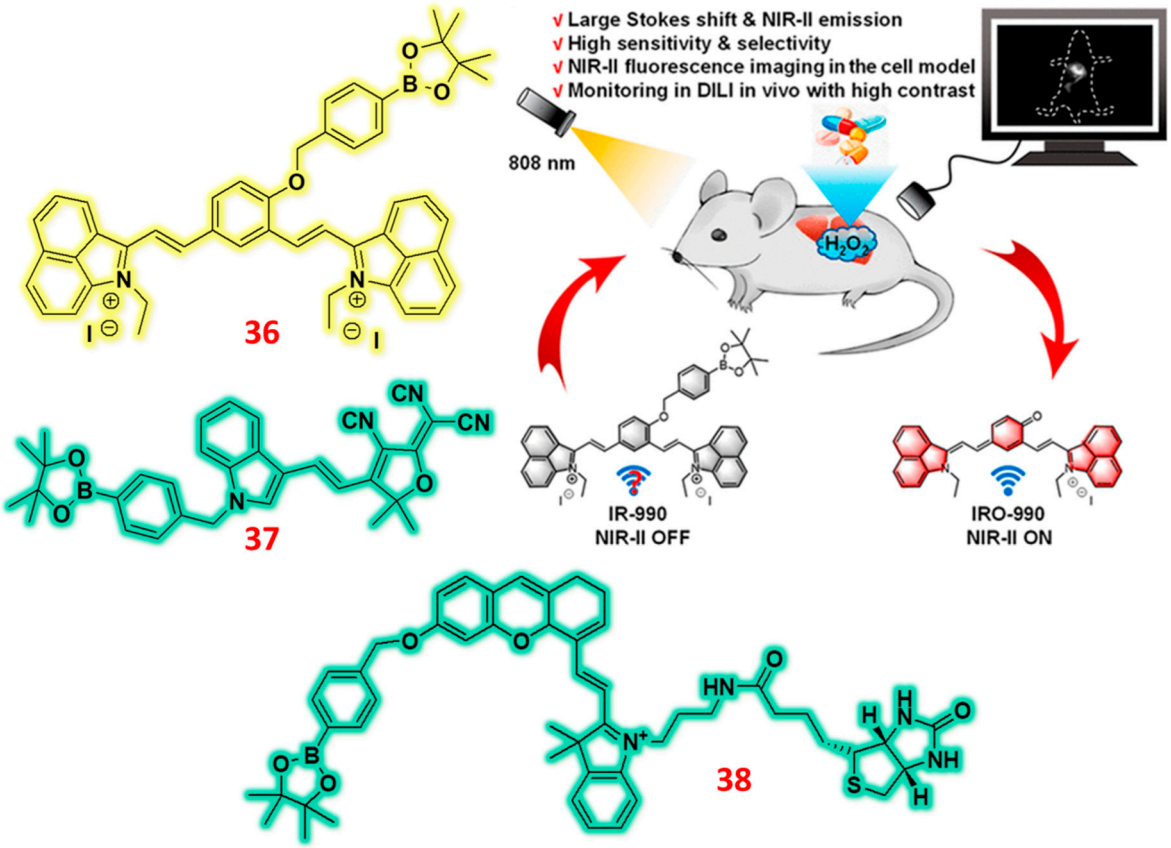

Figure 12. Structure of Indole based fluorescent probes (**36-38**) for the detection of H_2O_2 ions and monitoring of H_2O_2 in drug induced liver injury mice through probe **36**. Reproduced with permission from Refs. [85], Copyright, American Chemical Society.

2.8. Chromene Based Fluorescent Probes

Chromene is a crucial chromophore for creating new dyes with aggregation-induced emission (AIE) properties, specifically for near-infrared (NIR) applications in living organisms. Its significance lies in developing innovative dye structures and modifying existing ones for various uses. These include photoacoustic imaging, photothermal therapy, metal ion sensing, and drug delivery. Key objectives drive the design and modification of these dyes: creating novel crossbreeding skeletons to enhance dye performance, broadening the wavelength range for improved functionality, ensuring structural stability, and implementing strategies to increase brightness and overall efficacy. A chromene based NIR fluorescent probe was designed and examined for the sequential detection of H_2O_2 using SO_2 complexation with probe **39** [88]. As a colorimetric probe, 39 was first tested against different metal ions were there was an strong absorption peak for probe alone at 650 nm which was completely decreased upon the addition of HSO_3^- ions while other metal ions didn't show any changes in absorbance. Moreover, there was a color change observed from blue to colorless in naked eye. Upon fixing the excitation wavelength, probe had strong fluorescence emission at 685 nm but the strong emission was completely quenched upon the addition of HSO_3^- ions. Furthermore, sequential sensing studies were carried out for 39+HSO_3^- complexation against various analytes such as ROS, RNS and aminoacids. In colorimetric technique, probe 39 with HSO_3^- had weak absorbance and quenching of fluorescence emission but it was completely reversed upon the addition of H_2O_2 were the absorbance and fluorescence emission was restored to its natural position along with color change from colorless solution to blue in naked eye. The changes in absorbance and fluorescence emission was due to presence of HSO_3^- and H_2O_2, were upon the addition of HSO_3^- had 1,4-addition reaction that disappeared NIR emission but H_2O_2 addition underwent elimination reaction to reappear NIR emission to its original position. Another NIR fluorescent probe **40** was developed for

 doi:10.20944/preprints202507.0403.v1

the specific sensing of H_2O_2 for its application usages in wound healing process and clinical tests [89]. Before its spectroscopic examination, probe 40 was examined in presence and absence of H_2O_2 in absorbance spectra titration were 40 had absorption peak at 445 nm which was completely diminished in presence of H_2O_2 with a new absorption peak at 560 nm. Upon fixing the excitation wavelength for fluorimetric titration, probe 40 was evaluated against different analytes such as cations, anions, aminoacids, ROS and RNS. The probe 40 along with other analytes had weak fluorescence emission at 690 nm but presence of H_2O_2 alone had strong enhancement in fluorescence emission which clearly indicates that probe 40 with H_2O_2 recognition site could detect H_2O_2 at very fast sensitive against all other analytes. The fluorescence emission change was noted to be because of H_2O_2 presence which triggered the recognition site of fluorophore to enhance its emission selectively detecting H_2O_2. Furthermore, the two probes 39 and 40 was successfully utilized for its biological applications while probe 39 was proved to detect H_2O_2 in different food samples and also in MCF-7 living cells. Upon increasing the concentration of H_2O_2 in pre-treated cell lines with probe 39, firstly probe alone had weak fluorescence emission which was increased in presence of H_2O_2 that was visualized in red emission channel. Another probe 40 was used in detecting H_2O_2 against HACAT cell lines, wounded mouse and human diabetic foot. As discussed in spectroscopic titration techniques, probe 40 had weak emission at NIR region, so NIR emission was triggered using the addition of H_2O_2.

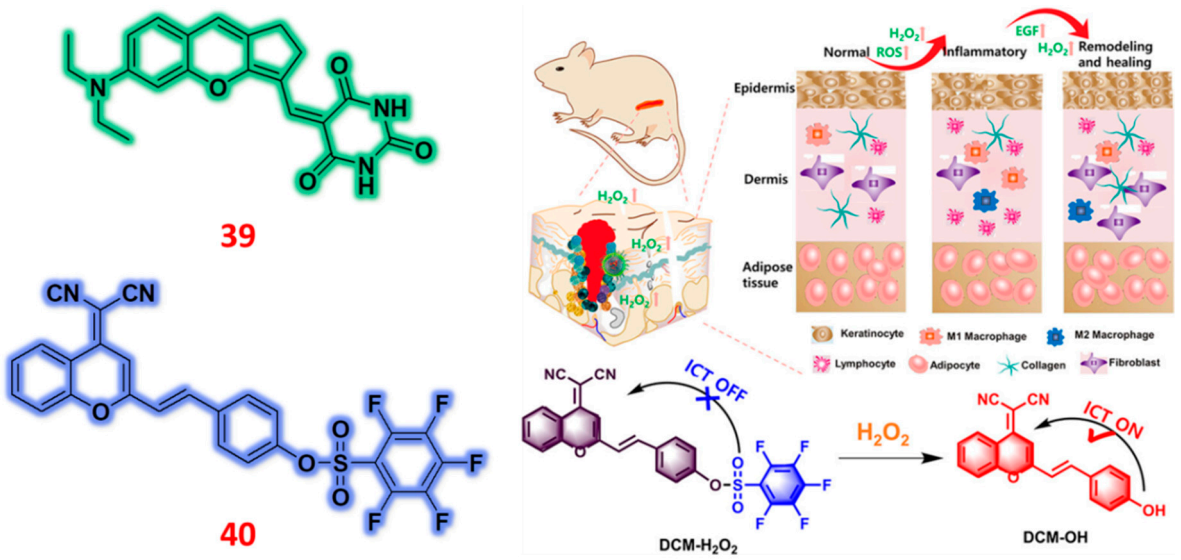

Figure 13. Structure of Chromene based fluorescent probes (**39 & 40**) for the detection of H_2O_2 ions and screening of H_2O_2 in wound healing process via mice model through probe **40**. Reproduced with permission from Refs. [89], Copyright, American Chemical Society.

2.9. Benzothiazole Based Fluorescent Probes

Due to their distinctive photophysical characteristics and wide uses, benzothiazole-based fluorescent probes are indispensable in materials science, chemistry, and biology. Essential tools in the domains of analytical chemistry, biology, and materials science, the probes show great degrees of brightness and stability in fluorescence. These technologies' great selectivity helps to exactly identify certain biomolecules. Their flexibility also allows customizing for other kinds of experimental configurations. These probes help environmental monitoring and quality control initiatives in analytical chemistry by allowing the sensitive identification and quantification of analytes. These instruments are crucial for diagnostics and bioimaging in biomedicine as they provide real-time molecular visualizing of cellular events and disease indicators. Moreover, including these components into smart materials offers chances to design responsive systems able to change their

 doi:10.20944/preprints202507.0403.v1

characteristics in reaction to environmental cues. Constant research and development of benzothiazole-based fluorescent probes show significant improvement, thereby enabling developments in early illness diagnosis, focused treatments, and the creation of novel materials with particular use in mind. Using an AIE-ESIPT technique for the specific detection of HSO_3^- and sequential detection of H_2O_2, Lijun Tang and colleagues have created a new fluorescent probe labeled as **41** [90]. For use in cell imaging, the detecting technique was improved yet further. With absorbance measured at 600 nm and emission at 650 nm, probe 41 first showed notable absorbance and fluorescence emission features, ascribed to the interaction of AIE and ESIPT systems. Strong absorption and emission were seen when probe 41 was tested against many analytes including HSO_3^- ions. Absorbance was clearly reduced and fluorescence quenched, nevertheless, in the presence of HSO_3^- ions. Under normal lighting, this was followed by a clear color shift from blue to colorless; under UV-365nm irradiation, from red to colorless. Sequential selectivity against many molecules—including reactive oxygen species (ROS), reactive nitrogen species (RNS), and amino acids—was achieved using the complexation system probe 41+HSO_3^-. In presence of H_2O_2, the weak absorption and quenching of fluorescence emission were effectively induced. Increasing the concentration of H_2O_2 helped to return the absorbance and emission to their natural level, therefore reversing the color change. The 1,4 Michael addition reaction involving HSO_3^- and the retro- Michael addition reaction enabled by H_2O_2 may be responsible for the selective detection of HSO_3^- and sequential detection of H_2O_2 within the complexation system. Different spectroscopic methods verified the complexation mechanism even more. Designed for selective detection of H_2O_2 in live cells, a benzothiazole derivative-based fluorescent probe **42** was created [91]. Acting as an AIE probe, Probe 42 had poor fluorescence emission at 604 nm alone. On treatment with many analytes, only hydrogen peroxide (H_2O_2) showed a notable increase in fluorescence intensity; the other analytes did not clearly affect emission. The H_2O_2 presence was blamed for the variations in fluorescence emission. Probe 42 showed a "turn-off" fluorescence effect before H_2O_2 was added; this effect was then triggered in the presence of H_2O_2 and produced a "turn-on" fluorescence response. Successful development of a multifunctional fluorescent probe 43 for sequential H_2O_2 detection and SO_2 detection is reported. By means of the induced SO_2 and H_2O_2 procedures, the produced probe **43** was essentially used in the application process for both physiological and pathological circumstances connected to human illnesses [92]. Probe 43 first underwent analysis with respect to many analytes, including biological and environmental species. The probe showed a significant absorption peak at 610 nm, which dropped with SO_2 ion injection. By contrast, the probe showed a drop in fluorescence intensity at 750 nm and an increase at 510 nm when the excitation wavelength was fixed. H_2O_2 was sensed sequentially using a complexation method. Along with a rise in fluorescence intensity at 750 nm and a drop at 510 nm, a concentration of H_2O_2 significantly raised the absorption peak at 610 nm. This unequivocally shows that in the presence of H_2O_2 both fluorescence emission and absorbance was restored. The reversibility cycle showed that the probe, in the presence and absence of SO_2/H_2O_2, displayed restoration of absorbance and fluorescence emission following alternating addition up to six times, therefore suggesting its possible importance in biological processes. Designed and built by Lei Yang and colleagues, a near-infrared (NIR) fluorescent probe known as probe **44** could detect hydrogen peroxide (H_2O_2) using a fluorimetric titration method [93]. The efficacy of the probe in precisely tracking drug-induced liver damage was duly underlined. Originally in phase, the probe 44 had a modest absorption peak at 510 nm. H_2O_2 added helped to intensify this peak. Subsequently, the absorbance investigations let one ascertain the excitation wavelength for fluorimetric titration. At 772 nm, probe 44 showed no fluorescence emission signal during titration using many analytes. But when treated with H_2O_2, fluorescence intensity significantly increased, producing a 41-fold increase in emission. Fluorescence intensity consistently increased as the concentration of H_2O_2 with respect to probe 44 ranged from 0 to 100 μM. Furthermore absent from the complexation mechanism was interference from other analytes. The elimination of the boronic acid ester group in the presence of H_2O_2 produced the noted alterations in emission that resulted in the introduction of hydroxyl groups in probe 44. This change increases fluorescence emission by means of the intramolecular charge

 doi:10.20944/preprints202507.0403.v1

transfer (ICT) mechanism. Furthermore, all the probes investigated in this context were efficiently used for biological purposes involving many cell lines and animal tissues for the H_2O_2 detection. Probe 41 first showed intense red fluorescence when interacting with MCF-7 cells; however, this fluorescence decreased with increasing HSO_3^- concentration. Indicating that probe 41 may alternatively detect HSO_3^-/ H_2O_2 in live cells, the identical complexation system showed a recovery of H_2O_2 fluorescence intensity. Tested against two different cell lines, A549 and HepG2, Probe 42 showed modest fluorescence in the green channel. On higher concentrations of H_2O_2, however, fluorescence emission was clearly increasing. Fluorescence emission in the green channel significantly increased as concentration ranged from 5 μM to 100 μM. In photoacoustical and cell imaging, probe 43 was a multifarious detector for SO_2 and H_2O_2. Probe 43 showed considerable emission in the red channel when Na_2SO_3 was added, starting off with mild emission. Moreover, especially in studies involving the HepG2 cell line, increasing concentrations of H_2O_2 clearly resulted in a significant increase in fluorescence emission in the red channel. In the photoacoustic investigation, probe 43 was assessed in tumor-bearing and inflammatory animal models both with and without Na_2SO_3/H_2O_2. Examining the probe 43 separately, we found a strong PA signal that was much reduced with NA_2SO_3's addition and then recovered following H_2O_2 addition. Within the framework of the HepG2 cell line and drug-induced liver damage tissue, a near infrared probe 44 displaying high fluorescence emission was effectively assessed against H_2O_2. For probe 44, the experimental findings showed a high degree of performance in identifying H_2O_2 levels in the cell lines. Probe 44 showed great sensitivity to H_2O_2 in the investigation of samples treated for drug-induced liver damage, therefore indicating its possible use as a visual diagnostic and therapeutic drug screening tool (Figure 14).

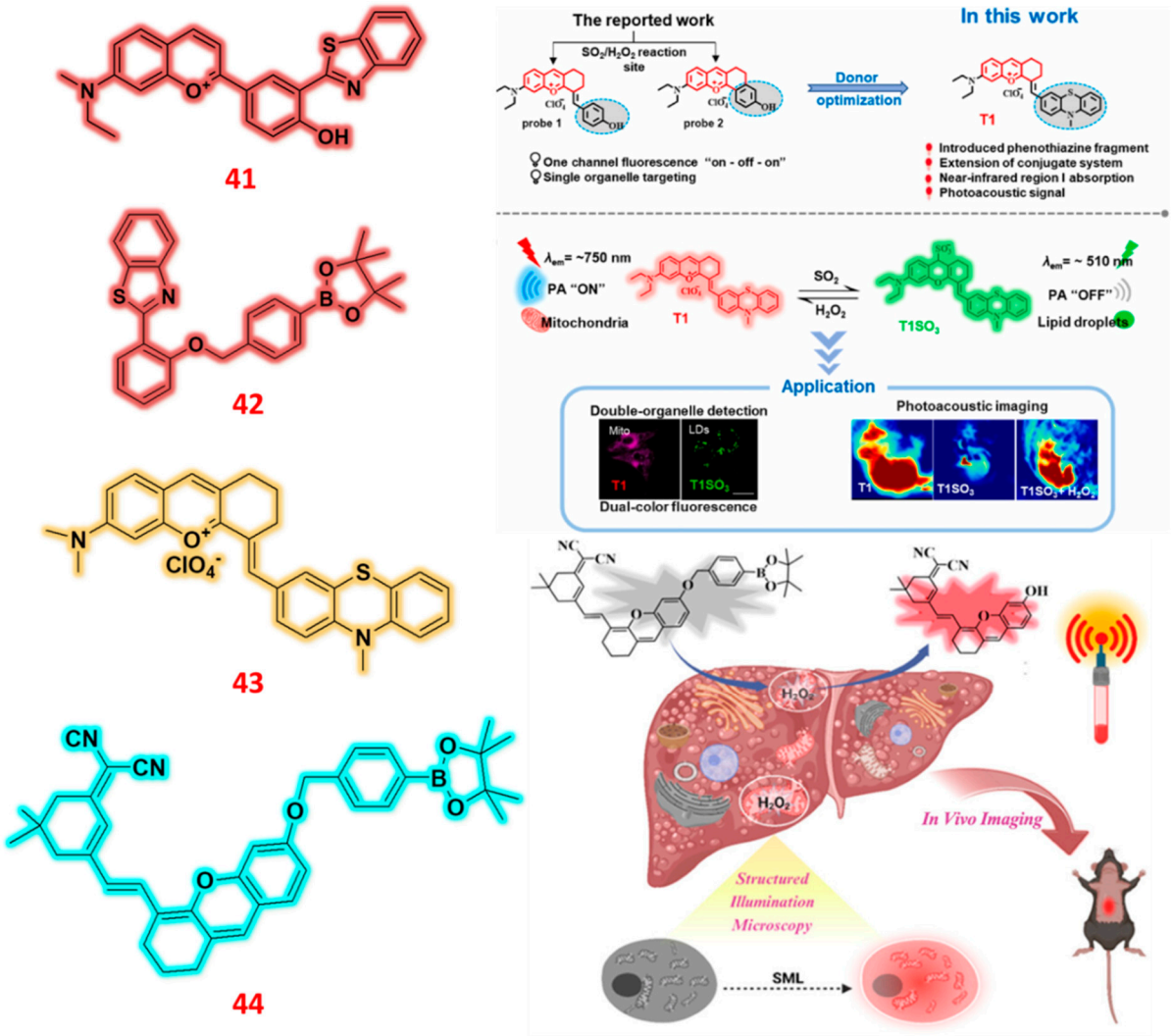

 doi:10.20944/preprints202507.0403.v1

Figure 14. Structure of Benzothiazole based fluorescent probes (**41-44**) for the specific detection of H_2O_2 ions and its graphical illustration diagrams representing probe **43** for its applications in double-organelle detection and photoacoustic imaging. Probe **44** was tested against mice model via in vivo imaging for the detection of H_2O_2. Reproduced with permission from Refs. [92][93], Copyright, Elsevier and American Chemical Society.

Table 1. The fluorescent probes derived developed from various fluorophores for their detection towards H_2O_2 and their detection limit, detection technique, applications in animal tissues/foodstuffs/plants, and cell imaging.

Probe	Derivative	Detection method	Analyte	LOD	Animal tissues/ Food samples	Cell imaging	Reference
1	TPA	F	H_2O_2	0.141 μmol/L	Living normal tissues and tumor	HeLa	[50]
2	TPA	F	H_2O_2	0.25 mM	-	HeLa	[51]
3	TPA	C/F	H_2O_2	62 nM	Acute epilepsy & Chronic epilepsy mice	PC12	[52]
4	TPA	F	H_2O_2	0.34 μmol/L	Inflammation and ferroptosis mice	HepG2	[53]
5	TPA	F	H_2O_2	2.84 μM	Zebrafish	HepG2	[54]
6	TPE	F	H_2O_2	-	Tobacco leaves	Orin apple calli cells	[55]
7	TPE	C/F	H_2O_2	3.52 μM	Sugar	MCF-7	[56]
8	Quinoline	C/F	H_2O_2	44.6 nM	Zebrafish	HepG2	[57]
9	Quinoline	C/F	H_2O_2	23.08 nM	Potato tissues, Milk and Chicken wing	-	[58]
10	Quinoline	C/F	H_2O_2	0.87 μM	-	HeLa	[59]
11	Quinolinium	F	H_2O_2	0.17 μM	Diabetic mice	HeLa, HCT116 and 4T1 cells	[60]
12	Quinolinium	F	H_2O_2	210 nM	RA mice	HeLa	[61]
13	Quinolinium	C/F	H_2O_2	0.17 μM	Mice	SH-SY5Y	[62]
14	Quinolinium	F	H_2O_2	13 nM	CIRI rat	SH-SY5Y	[63]
15	Pinacol	C/F	H_2O_2	40.2 nM	Zebrafish	Raw 264.7	[64]
16	Pinacol	F	H_2O_2	0.003 μmol/L	-	HeLa	[65]

 doi:10.20944/preprints202507.0403.v1

17	Pinacol	F	H_2O_2	-	Tumor-bearing mice	A375 cells	[66]
18	Pinacol	F	H_2O_2	49.74 nM	-	A549 cells	[67]
19	Pinacol	C/F	H_2O_2	386 nM & 16.8 nM	-	HeLa	[68]
20	Cinnamaldehyde	F	H_2O_2	-	-	HepG2	[69]
21	Hydroxybenzaldehyde	C/F	H_2O_2	1.02 mM	Zebrafish, mice and white wine, sugar samples	-	[70]
22	Carbaldehyde	C/F	H_2O_2	-	Cystitis mice	-	[71]
23	Benzaldehyde	F	H_2O_2	0.14 & 0.37 μm	Mice	HeLa	[72]
24	Carboxaldehyde	F	H_2O_2	112.6 nM	4T1 bearing tumor mice	4T1	[73]
25	Hydroxybenzaldehyde	F	H_2O_2	-	-	L-02 cells and HeLa, CT26 cells	[74]
26	Cinnamaldehyde	F	H_2O_2	0.36 μM	Tumor cell pyroptosis	4T1	[75]
27	Hemicyanine	F	H_2O_2	0.53 μM	HIRI and NAFL mice model	-	[76]
28	Hemicyanine	F	H_2O_2	0.38 μM	Mice tumor tissue	HeLa & A549 cells	[77]
29	Hemicyanine	C/F	H_2O_2	0.07 μM	Tomato leaves, stems, and roots	-	[78]
30	Hemicyanine	F	H_2O_2	0.14 μM	4T1 tumor-bearing mouse	4T1	[79]
31	Hemicyanine	C/F	H_2O_2	0.16 μM	PD-mice	SH-SY5Y	[80]
32	Hemicyanine	C/F	H_2O_2	0.361 mM	ApoE−/−/HF & ApoE−/−/HF/setanaxib group mice	LOX-1 & IL-1b	[81]
33	Dicyanoisophorone	F	H_2O_2	76 nM	Zebrafish	HepG2	[82]
34(i) (ii)	Dicyanoisophorone	F	H_2O_2	4.525 μM	Zebrafish	HeLa	[83]

 doi:10.20944/preprints202507.0403.v1

35 (i) (ii)	Dicyanomethylene	F	H_2O_2	-	DU-145 tumor-bearing mice	MCF-10A, MCF-7, and DU-145 cells	[84]
36	Indolium	C/F	H_2O_2	0.59 μM	APAP-induced liver injury mouse	HeLa	[85]
37	Indole	F	H_2O_2	25.2 nM	Zebrafish	A459 cells	[86]
38	Trimethylindole	C/F	H_2O_2	1.82×10^{-7} M	4T1 mice model	4T1 cells	[87]
39	Chromene	C/F	H_2O_2	2.157 μM	Liquor, Red wine, Sugar and Biscuit samples	MCF-7 cells	[88]
40	Chromene	C/F	H_2O_2	64 nM	Wounded mouse models	HeLa, HACAT	[89]
41	Benzothiazole	C/F	H_2O_2	0.152 μM	-	MCF-7 cells	[90]
42	Benzothiazole	F	H_2O_2	0.93 μM	-	A549 & Hep G2 cells	[91]
43	Benzopyrylium	C/F	H_2O_2	9.76×10^{-7} M	Tumor-bearing mice	Hep G2 cells	[92]
44	Benzopyranonitrile	F	H_2O_2	17 nM	Liver injury mice	L02 and HeLa cells	[93]

3. Conclusions

The development of fluorescent probes employing near-infrared (NIR) and aggregation-induced emission (AIE) technologies is under more and more attention by researchers all over. These probes are very well-liked for their capacity to do both qualitative and quantitative studies of a broad spectrum of molecules, including cations, anions, amino acids, enzymes, and other physiologically important compounds. This review focuses on scholarly publications released between 2021-2025 that describe the design and synthesis of creative NIR/AIE-based fluorescent probes derived from various fluorophores for the detection of hydrogen peroxide (H_2O_2) using both colorimetric and fluorimetric spectroscopic techniques.

The methods of detection used are investigated in this study, thereby defining the processes of action and studying the many biological uses. All of the applications—cell imaging, animal tissue analysis, food sample testing, plant research—have an eye on H_2O_2. Furthermore, we underline the chemical approaches used to enhance the NIR emission characteristics of these fluorescent probes, particularly with regard to cancer-related disorders. This overview mainly addresses NIR-based fluorescent probes based on Förster resonance energy transfer (FRET) that function as intramolecular charge transfer (ICT)-dependent activatable fluorophores and systems. Innovations in this field usually combine quenching pairs with NIR-emitting systems, which are coordinated by interactions with metal ions, enzymes, peptides, or amino acids acting as targeting agents. Specifically discussed

 doi:10.20944/preprints202507.0403.v1

is the important function of NIR/AIE fluorescent probes in the selective detection of H_2O_2 in complicated biological settings. These probes show remarkable sensitivity for reactive nitrogen species (RNS), reactive oxygen species (ROS), and many other analytes, hence lowering the detection limit and increasing the quantum yield. Although many NIR/AIE fluorescent probes included in this study show amazing characteristics including excellent usage in numerous animal tissues, food samples, plants, and a variety of cell imaging applications across many cell lines, there is still much room for improvement. Still difficult are issues related to short emission wavelengths, naked eye vision, and interference from other analytes, all of which might influence diagnosis attempts linked with different disorders.

Moreover, the search of focused H_2O_2 probes for different organelles—including lysosomes and mitochondria—has presented many difficulties. By means of continuous efforts of the scientific community, it is expected that answers to these problems would progressively surface; producing more sophisticated and focused fluorescent H_2O_2 probes. High-performance probes are projected to provide rather powerful instruments for H_2O_2 detection in subcellular organelles. Eventually, in vivo applications made possible by this development will help to clarify cellular processes and disease causes.

Author Contributions: G. Prabakaran: Writing – review & editing, Writing – original draft, Investigation, Conceptualization. S. Suguna: Writing – review & editing, Conceptualization. K.Velmurugan: Writing – review & editing, Writing – original draft, Investigation, Conceptualization.

Funding: There are no sources of funding to declare.

Data availability statement: No data was used for the research described in the article.

Conflicts of Interest: The authors declare that they have no known competing financial interests.

References

1. Yin, J.; Huang, L.; Wu, L.; Li, J.; James, T.D.; Lin, W. Small molecule based fluorescent chemosensors for imaging the microenvironment within specific cellular regions. *Chem. Soc. Rev.* **2021**, *50*, 12098–12150, doi:10.1039/D1CS00645B.
2. Zheng, Z.; Feng, S.; Gong, S.; Feng, G. Golgi-targetable fluorescent probe for ratiometric imaging of CO in cells and zebrafish. *Sensors Actuators B Chem.* **2021**, *347*, 130631, doi:10.1016/J.SNB.2021.130631.
3. Zhang, Y.; Yan, Y.; Xia, S.; Wan, S.; Steenwinkel, T.E.; Medford, J.; Durocher, E.; Luck, R.L.; Werner, T.; Liu, H. Cell Membrane-Specific Fluorescent Probe Featuring Dual and Aggregation-Induced Emissions. *ACS Appl. Mater. Interfaces* **2020**, *12*, 20172–20179, doi:10.1021/ACSAMI.0C00903.
4. Huang, H.; Pan, S.; Yuan, B.; Wang, N.; Shao, L.; Chen, Z.E.; Zhang, H.; Huang, W.Z. Recent Research Progress of Benzothiazole Derivative Based Fluorescent Probes for Reactive Oxygen (H2O2 HClO) and Sulfide (H2S) Recognition. *J. Fluoresc.* **2024**, 1–18, doi:10.1007/S10895-024-04016-W/METRICS.
5. Wang, C.; Wang, Y.; Wang, G.; Huang, C.; Jia, N. A new mitochondria-targeting fluorescent probe for ratiometric detection of H2O2 in live cells. *Anal. Chim. Acta* **2020**, *1097*, 230–237, doi:10.1016/J.ACA.2019.11.024.
6. Li, S.; Xiao, Y.; Chen, C.; Jia, L. Recent Progress in Organic Small-Molecule Fluorescent Probe Detection of Hydrogen Peroxide. *ACS Omega* **2022**, *7*, 15267–15274, doi:10.1021/ACSOMEGA.2C00117.
7. Song, X.; Bai, S.; He, N.; Wang, R.; Xing, Y.; Lv, C.; Yu, F. Real-Time Evaluation of Hydrogen Peroxide Injuries in Pulmonary Fibrosis Mice Models with a Mitochondria-Targeted Near-Infrared Fluorescent Probe. *ACS Sensors* **2021**, *6*, 1228–1239, doi:10.1021/ACSSENSORS.0C02519
8. Li, B.; Bian, C.; Yang, L.; Zhu, Y.; Li, Z.; Yu, M. Unveiling Cellular Microenvironments with a Near-Infrared Fluorescent Sensor: A Dual-Edge Tool for Cancer Detection and Drug Screening. *Anal. Chem.* **2024**, doi:10.1021/ACS.ANALCHEM.4C03155.
9. Jiang, C.; Huang, H.; Kang, X.; Yang, L.; Xi, Z.; Sun, H.; Pluth, M.D.; Yi, L. NBD-based synthetic probes for sensing small molecules and proteins: design, sensing mechanisms and biological applications. *Chem. Soc. Rev.* **2021**, *50*, 7436–7495, doi:10.1039/D0CS01096K.

 doi:10.20944/preprints202507.0403.v1

10. Wang, T.; Shi, X.; Xu, X.; Zhang, J.; Ma, Z.; Meng, C.; Jiao, D.; Wang, Y.; Chen, Y.; He, Z.; et al. Emerging prodrug and nano-drug delivery strategies for the detection and elimination of senescent tumor cells. *Biomaterials* **2025**, *318*, doi:10.1016/J.BIOMATERIALS.2025.123129.
11. Krishnendu, M.R.; Singh, S. Reactive oxygen species: Advanced detection methods and coordination with nanozymes. *Chem. Eng. J.* **2025**, *511*, doi:10.1016/J.CEJ.2025.161296.
12. Chaturvedi, V.; Kumari, R.; Sharma, P.; Pati, A.K. Diverse Fluorescent Probe Concepts for Detection and Monitoring of Reactive Oxygen Species. *Chem. - An Asian J.* **2025**, doi:10.1002/ASIA.202401524.
13. Lin, S.; Ye, C.; Lin, Z.; Huang, L.; Li, D. Recent progress of near-infrared fluorescent probes in the determination of reactive oxygen species for disease diagnosis. *Talanta* **2024**, *268*, doi:10.1016/J.TALANTA.2023.125264.
14. Gu, W.; Li, S.; Yang, Y.; Wang, S.; Li, K.; Zhao, Y.; Mu, J.; Chen, X. In vivo optical imaging of reactive oxygen species (ROS)-related non-cancerous diseases. *TrAC - Trends Anal. Chem.* **2023**, *169*, doi:10.1016/J.TRAC.2023.117360.
15. Fang, J.; Li, X.; Gao, C.; Tao, J.; Li, W.; Seidu, M.A.; Zhou, H. Oxidative cleavage of alkene: A new strategy to construct a mitochondria-targeted fluorescent probe for hydrogen peroxide imaging in vitro and in vivo. *Sensors Actuators B Chem.* **2023**, *395*, doi:10.1016/J.SNB.2023.134504.
16. Ye, Y.; Sun, J.; Tang, F.; Xie, R.; Wang, H.; Ding, A.; Pan, S.; Li, L. Mitochondria-Targeting BODIPY Probes for Imaging of Reactive Oxygen Species. *Adv. Sens. Res.* **2023**, *2*, doi:10.1002/ADSR.202300057.
17. Ye, S.; Hu, J.J.; Yang, D. Tandem Payne/Dakin Reaction: A New Strategy for Hydrogen Peroxide Detection and Molecular Imaging. *Angew. Chemie - Int. Ed.* **2018**, *57*, 10173–10177, doi:10.1002/ANIE.201805162.
18. Gough, D.R.; Cotter, T.G. Hydrogen peroxide: A Jekyll and Hyde signalling molecule. *Cell Death Dis.* **2011**, *2*, doi:10.1038/CDDIS.2011.96.
19. Winterbourn, C.C. Reconciling the chemistry and biology of reactive oxygen species. *Nat. Chem. Biol.* **2008**, *4*, 278–286, doi:10.1038/NCHEMBIO.85.
20. Rhee, S.G. H2O2, a necessary evil for cell signaling. *Science (80-.).* **2006**, *312*, 1882–1883, doi:10.1126/SCIENCE.1130481.
21. Sundaresan, M.; Yu, Z.-X.; Ferrans, V.J.; Irani, K.; Finkel, T. Requirement for Generation of H 2 O 2 for Platelet-Derived Growth Factor Signal Transduction . *Science (80-.).* **1995**, *270*, 296–299, doi:10.1126/SCIENCE.270.5234.296.
22. Srikun, D.; Albersa, A.E.; Chang, C.J. A dendrimer-based platform for simultaneous dual fluorescence imaging of hydrogen peroxide and pH gradients produced in living cells. *Chem. Sci.* **2011**, *2*, 1156–1165, doi:10.1039/C1SC00064K.
23. Lisanti, M.P.; Martinez-Outschoorn, U.E.; Lin, Z.; Pavlides, S.; Whitaker-Menezes, D.; Pestell, R.G.; Howell, A.; Sotgia, F. Hydrogen peroxide fuels aging, inflammation, cancer metabolism and metastasis: The seed and soil also needs "fertilizer." *Cell Cycle* **2011**, *10*, 2440–2449, doi:10.4161/CC.10.15.16870.
24. Miller, E.W.; Tulyanthan, O.; Isacoff, E.Y.; Chang, C.J. Molecular imaging of hydrogen peroxide produced for cell signaling. *Nat. Chem. Biol.* **2007**, *3*, 263–267, doi:10.1038/NCHEMBIO871.
25. Rezende, F.; Brandes, R.P.; Schröder, K. Detection of hydrogen peroxide with fluorescent dyes. *Antioxidants Redox Signal.* **2018**, *29*, 585–602, doi:10.1089/ARS.2017.7401.
26. Zhou, J.; Ma, H. Design principles of spectroscopic probes for biological applications. *Chem. Sci.* **2016**, *7*, 6309–6315, doi:10.1039/C6SC02500E.
27. Li, X.; Gao, X.; Shi, W.; Ma, H. Design strategies for water-soluble small molecular chromogenic and fluorogenic probes. *Chem. Rev.* **2014**, *114*, 590–659, doi:10.1021/CR300508P.
28. Carter, K.P.; Young, A.M.; Palmer, A.E. Fluorescent sensors for measuring metal ions in living systems. *Chem. Rev.* **2014**, *114*, 4564–4601, doi:10.1021/CR400546E.
29. Wu, X.; Shao, A.; Zhu, S.; Guo, Z.; Zhu, W. A novel colorimetric and ratiometric NIR fluorescent sensor for glutathione based on dicyanomethylene-4H-pyran in living cells. *Sci. China Chem.* **2016**, *59*, 62–69, doi:10.1007/S11426-015-5490-Y/METRICS.
30. Koide, Y.; Urano, Y.; Hanaoka, K.; Piao, W.; Kusakabe, M.; Saito, N.; Terai, T.; Okabe, T.; Nagano, T. Development of NIR fluorescent dyes based on Si-rhodamine for in vivo imaging. *J. Am. Chem. Soc.* **2012**, *134*, 5029–5031, doi:10.1021/JA210375E.

 doi:10.20944/preprints202507.0403.v1

31. Yang, X.; Shi, C.; Tong, R.; Qian, W.; Zhau, H.E.; Wang, R.; Zhu, G.; Cheng, J.; Yang, V.W.; Cheng, T.; et al. Near Infrared Heptamethine Cyanine Dye-Mediated Cancer Imaging. *Clin. Cancer Res.* **2010**, *16*, 2833, doi:10.1158/1078-0432.CCR-10-0059.
32. Ahn, H.Y.; Yao, S.; Wang, X.; Belfield, K.D. Near-infrared-emitting squaraine dyes with high 2PA cross-sections for multiphoton fluorescence imaging. *ACS Appl. Mater. Interfaces* **2012**, *4*, 2847–2854, doi:10.1021/AM300467W.
33. Li, M.; Xia, J.; Tian, R.; Wang, J.; Fan, J.; Du, J.; Long, S.; Song, X.; Foley, J.W.; Peng, X. Near-Infrared Light-Initiated Molecular Superoxide Radical Generator: Rejuvenating Photodynamic Therapy against Hypoxic Tumors. *J. Am. Chem. Soc.* **2018**, *140*, 14851–14859, doi:10.1021/JACS.8B08658.
34. Wu, D.; Chen, L.; Xu, Q.; Chen, X.; Yoon, J. Design principles, sensing mechanisms, and applications of highly specific fluorescent probes for HOCl/OCl-. *Acc. Chem. Res.* **2019**, *52*, 2158–2168, doi:10.1021/ACS.ACCOUNTS.9B00307.
35. Prabakaran, G.; Xiong, H. Unravelling the recent advancement in fluorescent probes for detection against reactive sulfur species (RSS) in foodstuffs and cell imaging. *Food Chem.* **2025**, *464*, 141809, doi:10.1016/J.FOODCHEM.2024.141809.
36. Prabakaran, G.; David, C.I.; Nandhakumar, R. A review on pyrene based chemosensors for the specific detection on d-transition metal ions and their various applications. *J. Environ. Chem. Eng.* **2023**, *11*, 109701, doi:10.1016/J.JECE.2023.109701.
37. Immanuel David, C.; Prabakaran, G.; Nandhakumar, R. Recent approaches of 2HN derived fluorophores on recognition of Al3+ ions: A review for future outlook. *Microchem. J.* **2021**, *169*, 106590, doi:10.1016/J.MICROC.2021.106590.
38. Yuan, L.; Lin, W.; Zheng, K.; Zhu, S. FRET-based small-molecule fluorescent probes: Rational design and bioimaging applications. *Acc. Chem. Res.* **2013**, *46*, 1462–1473, doi:10.1021/AR300273V.
39. Lou, Z.; Li, P.; Han, K. Redox-responsive fluorescent probes with different design strategies. *Acc. Chem. Res.* **2015**, *48*, 1358–1368, doi:10.1021/ACS.ACCOUNTS.5B00009.
40. A. Prasanna de Silva, *; H. Q. Nimal Gunaratne; Thorfinnur Gunnlaugsson; Allen J. M. Huxley; Colin P. McCoy; Jude T. Rademacher, and; Rice, T.E. Signaling Recognition Events with Fluorescent Sensors and Switches. *Chem. Rev.* **1997**, *97*, 1515–1566, doi:10.1021/CR960386P.
41. Valeur, B.; Leray, I. Design principles of fluorescent molecular sensors for cation recognition. *Coord. Chem. Rev.* **2000**, *205*, 3–40, doi:10.1016/S0010-8545(00)00246-0.
42. Prabakaran, G.; Velmurugan, K.; David, C.I.; Nandhakumar, R. Role of Förster Resonance Energy Transfer in Graphene-Based Nanomaterials for Sensing. *Appl. Sci. 2022, Vol. 12, Page 6844* **2022**, *12*, 6844, doi:10.3390/APP12146844.
43. Chua, M.H.; Hui, B.Y.K.; Chin, K.L.O.; Zhu, Q.; Liu, X.; Xu, J. Recent advances in aggregation-induced emission (AIE)-based chemosensors for the detection of organic small molecules. *Mater. Chem. Front.* **2023**, *7*, 5561–5660, doi:10.1039/D3QM00679D.
44. Sun, W.; Li, M.; Fan, J.; Peng, X. Activity-Based Sensing and Theranostic Probes Based on Photoinduced Electron Transfer. *Acc. Chem. Res.* **2019**, *52*, 2818–2831, doi:10.1021/ACS.ACCOUNTS.9B00340,.
45. Chi, W.; Chen, J.; Liu, W.; Wang, C.; Qi, Q.; Qiao, Q.; Tan, T.M.; Xiong, K.; Liu, X.; Kang, K.; et al. A General Descriptor Δ e Enables the Quantitative Development of Luminescent Materials Based on Photoinduced Electron Transfer. *J. Am. Chem. Soc.* **2020**, *142*, 6777–6785, doi:10.1021/JACS.0C01473.
46. Lee, M.H.; Kim, J.S.; Sessler, J.L. Small molecule-based ratiometric fluorescence probes for cations, anions, and biomolecules. *Chem. Soc. Rev.* **2015**, *44*, 4185–4191, doi:10.1039/C4CS00280F.
47. Zheng, W.L.; Zhou, Z.Y.; Zhu, T.; Zou, Z.X.; Shan, Q.F.; Huang, Q.; Wang, G.; Wang, Y. Construction of ICT-based fluorescence probes for the imaging of biothios. *Microchem. J.* **2025**, *210*, 112968, doi:10.1016/J.MICROC.2025.112968.
48. Pavadai, R.; Pavadai, N.; Palanisamy, R.; Amalraj, A.; Arivazhagan, M.; Honnu, G.; Kityakarn, S.; Thongmee, S.; Khumphon, J.; Khamboonrueang, D.; et al. Recent Trends and Future Challenges of Metal-Organic Framework-Based optical and electro-chemical sensing platforms for the Ultra-sensitive detection of biomarkers and environmental Contaminants: A review (Year − 2023 & 2024). *Microchem. J.* **2025**, *210*, doi:10.1016/j.microc.2025.112937.

 doi:10.20944/preprints202507.0403.v1

49. Udhayakumari, D. Mechanistic Innovations in Fluorescent Chemosensors for Detecting Toxic Ions: PET, ICT, ESIPT, FRET and AIE Approaches. *J. Fluoresc.* **2024**, 1–30, doi:10.1007/S10895-024-03843.
50. Fan, L.; Zan, Q.; Wang, X.; Wang, S.; Zhang, Y.; Dong, W.; Shuang, S.; Dong, C. A Mitochondria-Specific Orange/Near-Infrared-Emissive Fluorescent Probe for Dual-Imaging of Viscosity and H2O2 in Inflammation and Tumor Models. *Chinese J. Chem.* **2021**, *39*, 1303–1309, doi:10.1002/CJOC.202000725.
51. Wu, Q.; Li, Y.; Li, Y.; Wang, D.; Tang, B.Z. Hydrogen peroxide-responsive AIE probe for imaging-guided organelle targeting and photodynamic cancer cell ablation. *Mater. Chem. Front.* **2021**, *5*, 3489–3496, doi:10.1039/D1QM00328C.
52. Li, S.; Wang, P.; Ye, M.; Yang, K.; Cheng, D.; Mao, Z.; He, L.; Liu, Z. Cysteine-Activatable Near-Infrared Fluorescent Probe for Dual-Channel Tracking Lipid Droplets and Mitochondria in Epilepsy. *Anal. Chem.* **2023**, *95*, 5133–5141, doi:10.1021/ACS.ANALCHEM.3C00226
53. Tian, X.; Cheng, J.; Yang, L.; Li, Z.; Yu, M. A NIR Dual-Channel Fluorescent Probe for Fluctuations of Intracellular Polarity and H2O2 and Its Applications for the Visualization of Inflammation and Ferroptosis. *Chem. Biomed. Imaging* **2024**, *2*, 518–525, doi:10.1021/CBMI.3C00123
54. Li, J.; Kang, X.; Liu, N.; Zhang, A.; Li, L.; Zhao, X.; Li, Y.; Zhou, H.; Deng, Y.; Peng, C.; et al. A robust H2O2-responsive AIEgen with multiple-task performance: Achieving food analysis, visualization of dual organelles and diagnosis of liver injury. *Biosens. Bioelectron.* **2025**, *276*, 117276, doi:10.1016/J.BIOS.2025.117276.
55. Yin, Y.; Wang, G.; Liu, Y.; Wang, X.F.; Gao, W.; Zhang, S.; You, C. Simple Phenotypic Sensor for Visibly Tracking H2O2Fluctuation to Detect Plant Health Status. *J. Agric. Food Chem.* **2022**, *70*, 10058–10064, doi:10.1021/ACS.JAFC.2C02170
56. Li, Y.; Huang, Y.; Sun, X.; Zhong, K.; Tang, L. An AIE mechanism-based fluorescent probe for relay recognition of HSO3−/H2O2 and its application in food detection and bioimaging. *Talanta* **2023**, *258*, 124412, doi:10.1016/J.TALANTA.2023.124412.
57. Wang, Y.; Li, S.; Zhu, X.; Shi, X.; Liu, X.; Zhang, H. A novel H2O2 activated NIR fluorescent probe for accurately visualizing H2S fluctuation during oxidative stress. *Anal. Chim. Acta* **2022**, *1202*, 339670, doi:10.1016/J.ACA.2022.339670.
58. Chen, X.; He, D.; Shentu, J.; Yang, S.; Yang, Y.; Wang, Y.; Zhang, R.; Wang, K.; Qian, J.; Long, L. Smartphone-assisted colorimetric and near-infrared ratiometric fluorescent sensor for on-spot detection of H2O2 in food samples. *Chem. Eng. J.* **2023**, *472*, 144900, doi:10.1016/J.CEJ.2023.144900.
59. Liu, F.T.; Wang, S.; Wang, Y.P.; Jiang, P.F.; Miao, J.Y.; Zhao, B.X.; Lin, Z.M. A near-infrared fluorescent probe based FRET for ratiometric sensing of H2O2 and viscosity in live cells. *Talanta* **2024**, *275*, 126135, doi:10.1016/J.TALANTA.2024.126135.
60. Li, C.Y.; Wang, W.X.; Jiang, W.L.; Mao, G.J.; Tan, M.; Fei, J.; Li, Y. Monitoring the fluctuation of hydrogen peroxide in diabetes and its complications with a novel near-infrared fluorescent probe. *Anal. Chem.* **2021**, *93*, 3301–3307, doi:10.1021/ACS.ANALCHEM.0C05364
61. Zhong, S.; Huang, S.; Feng, B.; Luo, T.; Chu, F.; Zheng, F.; Zhu, Y.; Chen, F.; Zeng, W. An ESIPT-based AIE fluorescent probe to visualize mitochondrial hydrogen peroxide and its application in living cells and rheumatoid arthritis. *Org. Biomol. Chem.* **2023**, *21*, 5063–5071, doi:10.1039/D3OB00546A.
62. Wang, X.; Iyaswamy, A.; Xu, D.; Krishnamoorthi, S.; Sreenivasmurthy, S.G.; Yang, Y.; Li, Y.; Chen, C.; Li, M.; Li, H.W.; et al. Real-Time Detection and Visualization of Amyloid-β Aggregates Induced by Hydrogen Peroxide in Cell and Mouse Models of Alzheimer's Disease. *ACS Appl. Mater. Interfaces* **2023**, *15*, 39–47, doi:10.1021/ACSAMI.2C07859
63. Fang, C.; Deng, Q.; Zhao, K.; Zhou, Z.; Zhu, X.; Liu, F.; Yin, P.; Liu, M.; Li, H.; Zhang, Y.; et al. Fluorescent Probe for Investigating the Mitochondrial Viscosity and Hydrogen Peroxide Changes in Cerebral Ischemia/Reperfusion Injury. *Anal. Chem.* **2024**, *96*, 3436–3444, doi:10.1021/ACS.ANALCHEM.3C04781
64. Chen, M.; Liang, Z.; Zeng, G.; Wang, Y.; Mai, Z.; Chen, X.; Wu, G.; Chen, T. An ESIPT-based NIR-emitting ratiometric fluorescent probe for monitoring hydrogen peroxide in living cells and zebrafish. *Dye. Pigment.* **2022**, *198*, 109995, doi:10.1016/J.DYEPIG.2021.109995.
65. An, B.; Pang, S.; Zhang, Y.; Wei, N. A novel near-infrared fluorescent probe for visualization of intracellular hydrogen peroxide. *Front. Chem.* **2022**, *10*, 1025723, doi:10.3389/FCHEM.2022.1025723.

 doi:10.20944/preprints202507.0403.v1

66. Peng, H.; Wang, T.; Li, G.; Huang, J.; Yuan, Q. Dual-Locked Near-Infrared Fluorescent Probes for Precise Detection of Melanoma via Hydrogen Peroxide–Tyrosinase Cascade Activation. *Anal. Chem.* **2022**, *94*, 1070–1075, doi:10.1021/ACS.ANALCHEM.1C04058
67. Tong, L.; Yang, Y.; Zhang, L.; Tao, J.; Sun, B.; Song, C.; Qi, M.; Yang, F.; Zhao, M.; Jiang, J. Design, Synthesis of Hydrogen Peroxide Response AIE Fluorescence Probes Based on Imidazo [1,2-a] Pyridine. *Molecules* **2024**, *29*, 882, doi:10.3390/MOLECULES29040882/S1.
68. He, Q.; Zang, S.; Zeng, Y.; Wang, B.; Song, X. A bifunctional fluorescent probe for dual-channel detection of H2O2 and HOCl in living cells. *Spectrochim. Acta Part A Mol. Biomol. Spectrosc.* **2025**, *328*, 125464, doi:10.1016/J.SAA.2024.125464.
69. Zheng, A.; Liu, H.; Gao, X.; Xu, K.; Tang, B. A Mitochondrial-Targeting Near-Infrared Fluorescent Probe for Revealing the Effects of Hydrogen Peroxide and Heavy Metal Ions on Viscosity. *Anal. Chem.* **2021**, *93*, 9244–9249, doi:10.1021/ACS.ANALCHEM.1C01511
70. Song, Q.; Zhou, B.; Zhang, D.; Chi, H.; Jia, H.; Zhu, P.; Zhang, Z.; Meng, Q.; Zhang, R. A reversible near-infrared fluorescence probe for the monitoring of HSO3−/H2O2-regulated cycles in vivo. *New J. Chem.* **2021**, *45*, 19011–19018, doi:10.1039/D1NJ03507J.
71. Zhang, X.; Chen, Y.; He, H.; Wang, S.; Lei, Z.; Zhang, F. ROS/RNS and Base Dual Activatable Merocyanine-Based NIR-II Fluorescent Molecular Probe for in vivo Biosensing. *Angew. Chemie* **2021**, *133*, 26541–26545, doi:10.1002/ANGE.202109728.
72. Wang, W.X.; Chao, J.J.; Wang, Z.Q.; Liu, T.; Mao, G.J.; Yang, B.; Li, C.Y. Dual Key-Activated Nir-I/II Fluorescence Probe for Monitoring Photodynamic and Photothermal Synergistic Therapy Efficacy. *Adv. Healthc. Mater.* **2023**, *12*, 2301230, doi:10.1002/ADHM.202301230.
73. Peng, Z.; Cui, M.; Chu, J.; Chen, J.; Wang, P. A novel AIE fluorescent probe for the detection and imaging of hydrogen peroxide in living tumor cells and in vivo. *Bioorg. Chem.* **2024**, *150*, 107592, doi:10.1016/J.BIOORG.2024.107592.
74. Chao, L.; Aodeng, G.; Ga, L.; Ai, J. Put one make three: Multifunctional near-infrared fluorescent probe for simultaneous detection of viscosity, polarity, SO2/H2O2. *Microchem. J.* **2025**, *208*, 112535, doi:10.1016/J.MICROC.2024.112535.
75. Deng, M.; Wang, P.; Zhai, Z.; Liu, Y.; Cheng, D.; He, L.; Li, S. A Triple-Responsive and Dual-NIR Emissive Fluorescence Probe for Precise Cancer Imaging and Therapy by Activating Pyroptosis Pathway. *Anal. Chem.* **2025**, *97*, 2998–3008, doi:10.1021/ACS.ANALCHEM.4C06015
76. Zan, Q.; Zhao, K.; Li, R.; Yang, Y.; Yang, X.; Li, W.; Zhang, G.; Dong, C.; Shuang, S.; Fan, L. Mitochondria-Targetable Near-Infrared Fluorescent Probe for Visualization of Hydrogen Peroxide in Lung Injury, Liver Injury, and Tumor Models. *Anal. Chem.* **2024**, *96*, 10488–10495, doi:10.1021/ACS.ANALCHEM.3C05479
77. Yin, N.; Wang, Y.; Qin, G.; Wang, M.; Tang, J.; Yao, X.; Xu, Q.; Yoon, J. A mitochondria-targeted fluorescent probe for revealing H2O2 elevation modulated by basal HClO in HeLa and A549 cells. *Sensors Actuators B Chem.* **2024**, *419*, 136419, doi:10.1016/J.SNB.2024.136419.
78. Jin, Z.; Song, L.; Yang, X.; Wang, Y.; Niu, N.; Chen, L. Development of a near-infrared fluorescent probe for in situ monitoring of hydrogen peroxide in plants. *Spectrochim. Acta Part A Mol. Biomol. Spectrosc.* **2025**, *339*, 126267, doi:10.1016/J.SAA.2025.126267.
79. Zhong, L.; Wang, Y.; Hao, Q.; Liu, H. A Hydrogen Peroxide Responsive Biotin-Guided Near-Infrared Hemicyanine-Based Fluorescent Probe for Early Cancer Diagnosis. *Chemosensors* **2025**, *13*, 104, doi:10.3390/CHEMOSENSORS13030104/S1.
80. Guo, L.; Li, X.; Xie, S.; Su, B.; Yang, N.; Wang, B.; Ma, S.; Li, L.; Yan, L.; Zhang, B.; et al. Double-locked probe for NIRF/PA imaging mitochondrial H2O2 and viscosity in Parkinson's disease. *Sensors Actuators B Chem.* **2025**, *426*, 137104, doi:10.1016/J.SNB.2024.137104.
81. Wang, H.; Guo, J.; Xiu, T.; Tang, Y.; Li, P.; Zhang, W.; Zhang, W.; Tang, B. H2O2 accumulation promoting internalization of ox-LDL in early atherosclerosis revealed via a synergistic dual-functional NIR fluorescence probe. *Chem. Sci.* **2024**, *16*, 345–353, doi:10.1039/D4SC05546B.
82. Chunpo, G.; Yan, Y.; Pengfei, T.; Hu, S.; Yibo, J.; Yuyang, S.; Yun, Y.; Feng, R. A NIR fluorescent probe for the in vitro and in vivo selective detection of hydrogen peroxide. *Sensors Actuators B Chem.* **2022**, *350*, 130831, doi:10.1016/J.SNB.2021.130831.

 doi:10.20944/preprints202507.0403.v1

83. Wu, Y.; Jing, F.; Huang, H.; Wang, H.; Chen, S.; Fan, W.; Li, Y.; Wang, L.; Wang, Y.; Hou, S. A near-infrared fluorescent probe for tracking endogenous and exogenous H2O2 in cells and zebrafish. *Spectrochim. Acta Part A Mol. Biomol. Spectrosc.* **2023**, *302*, 123158, doi:10.1016/J.SAA.2023.123158.
84. He, P.; Deng, X.; Xu, B.; Xie, B.; Zou, W.; Zhou, H.; Dong, C. Development of Highly Efficient Estrogen Receptor β-Targeted Near-Infrared Fluorescence Probes Triggered by Endogenous Hydrogen Peroxide for Diagnostic Imaging of Prostate Cancer. *Molecules* **2023**, *28*, 2309, doi:10.3390/MOLECULES28052309/S1.
85. Tian, Y.; Liu, S.; Cao, W.; Wu, P.; Chen, Z.; Xiong, H. H2O2-Activated NIR-II Fluorescent Probe with a Large Stokes Shift for High-Contrast Imaging in Drug-Induced Liver Injury Mice. *Anal. Chem.* **2022**, *94*, 11321–11328, doi:10.1021/ACS.ANALCHEM.2C02052
86. Jain, N.; Sonawane, P.M.; Roychaudhury, A.; Park, S.J.; An, J.; Kim, C.H.; Nimse, S.B.; Churchill, D.G. An indole–based near–infrared fluorescent "Turn–On" probe for H2O2: Selective detection and ultrasensitive imaging of zebrafish gallbladder. *Talanta* **2024**, *269*, 125459, doi:10.1016/J.TALANTA.2023.125459.
87. Zhong, D.; Xiong, S.; Zhang, Y.; Cui, M.; Liu, L.; Xu, Y.; Wang, P.; Zhang, W. H2O2-activated NIR fluorescent probe with tumor targeting for cell imaging and fluorescent-guided surgery. *Sensors Actuators B Chem.* **2024**, *418*, 136249, doi:10.1016/J.SNB.2024.136249.
88. Tian, L.; Sun, X.; Zhou, L.; Zhong, K.; Li, S.; Yan, X.; Tang, L. Reversible colorimetric and NIR fluorescent probe for sensing SO2/H2O2 in living cells and food samples. *Food Chem.* **2023**, *407*, 135031, doi:10.1016/J.FOODCHEM.2022.135031.
89. Luo, X.; Cheng, S.; Zhang, W.; Dou, K.; Wang, R.; Yu, F. Near-Infrared Fluorescence Probe for Indication of the Pathological Stages of Wound Healing Process and Its Clinical Application. *ACS Sensors* **2024**, *9*, 810–819, doi:10.1021/ACSSENSORS.3C02147
90. Huang, Y.; Li, Y.; Huang, X.; Tang, L.; Yan, X. A novel "AIE+ESIPT" mechanism-based fluorescent probe for visual alternating recognition of HSO3−/H2O2 and its HSO3− detection in food samples. *Dye. Pigment.* **2024**, *222*, 111901, doi:10.1016/J.DYEPIG.2023.111901.
91. Shi, D.; Yang, Y.; Tong, L.; Zhang, L.; Yang, F.; Tao, J.; Zhao, M. A Novel Benzothiazole-Based Fluorescent AIE Probe for the Detection of Hydrogen Peroxide in Living Cells. *Molecules* **2024**, *29*, 5181, doi:10.3390/MOLECULES29215181/S1.
92. Zhu, Y.; Wang, J.; Ni, Y.; Rao, Q.; Zhu, X.; Yu, J.; Wang, S.; Zhou, H. A multifunctionally reversible detector: Photoacoustic and dual-channel fluorescence sensing for SO2/H2O2. *Anal. Chim. Acta* **2023**, *1263*, 341181, doi:10.1016/J.ACA.2023.341181.
93. Zheng, H.; Peng, W.; Liu, M.; Li, M.; Li, W.; Xing, J.; Shi, P.; Wang, Q.; Zhang, S.; Yang, L. Super-Resolution Mitochondrial Fluorescent Probe for Accurate Monitoring of Drug-Induced Liver Injury. *Anal. Chem.* **2025**, doi:10.1021/ACS.ANALCHEM.4C06168.

Biographies

Dr. Prabakaran Gunasekaran obtained his Ph.D. degree from Karunya Institute of Technology and Sciences, Deemed to be University, Tamilnadu, India. Since 2024, he's working as Postdoctoral research fellow in Institute for Advanced Study (IAS), Shenzhen University, China. His current research is focused on the design and synthesis of NIR/AIE based fluorescent probes for detection of analytes and their practical, biological applications.

Dr. Suguna Sivasubramanian obtained his Ph.D. degree from Karunya Institute of Technology and Sciences, Deemed to be University, Tamilnadu, India. Her current research focused on Synthesis of Organic fluorescent chemosensors for metal ion detection and their real time applications and bio imaging.

Dr. Krishnasamy Velmurugan received his Ph.D. degree from Karunya Institute of Technology and Sciences, Deemed to be University, Tamilnadu, India. After he joined as a postdoctoral researcher at Xi'an Jiaotong University, P. R. China in 2017. Currently, he is a postdoctoral researcher at Nanjing University of Aeronautics and Astronautics (NUAA), P. R. China, and his research interests focus on supramolecular chiral self-assemblies and functional materials.

 doi:10.20944/preprints202507.0403.v1